

“MMHT” PDF Update

Robert Thorne

September 17th 2019



University College London

With Shaun Bailey, Tom Cridge, Lucian Harland-Lang, Alan Martin and
Ricky Nathvani

I will outline updates in the “MMHT” PDF approach.

Inclusion of new LHC data sets - largely electroweak processes, particularly precise ATLAS W, Z 7 TeV results. Implications for strange with NNLO corrections to dimuon production.

Extended parameterisation, including \bar{d}/\bar{u} and eigenvectors sets.

Problems with correlated uncertainties - differential top data.

Completion and release of MMHT2015 PDFs with QED corrections.

Brief recap – MMHT preliminary set (2016) - fit to new hadron collider (mainly LHC) data

Fit new LHCb data at 7 and 8 TeV, $W + c$ jets from CMS, CMS $W^{+,-}$ data, and also the final e asymmetry data from D0.

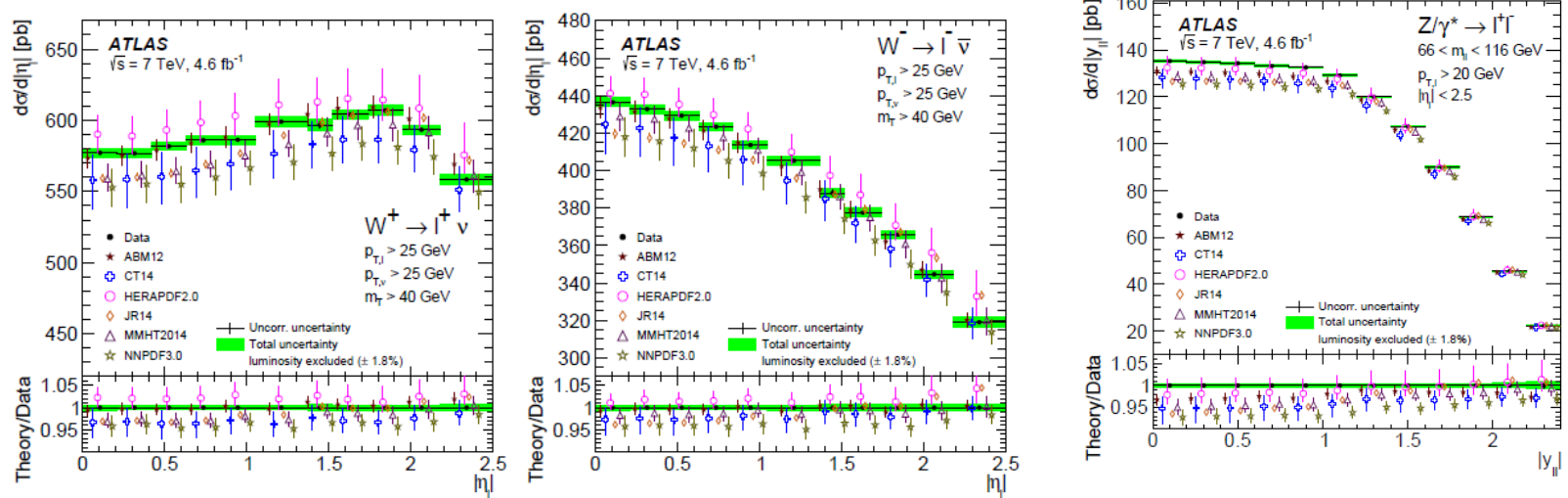
	no. points	NLO χ^2_{pred}	NLO χ^2_{new}	NNLO χ^2_{pred}	NNLO χ^2_{new}
$\sigma_{t\bar{t}}$ Tevatron +CMS+ATLAS	18	19.6	20.5	14.7	15.5
LHCb 7 TeV $W + Z$	33	50.1	45.4	46.5	42.9
LHCb 8 TeV $W + Z$	34	77.0	58.9	62.6	59.0
LHCb 8TeV e	17	37.4	33.4	30.3	28.9
CMS 8 TeV W	22	32.6	18.6	34.9	20.5
CMS 7 TeV $W + c$	10	8.5	10.0	8.7	8.0
D0 e asymmetry	13	22.2	21.5	27.3	25.8
total	3738/3405	4375.9	4336.1	3741.5	3723.7

Predictions good, and no real tension with other data when refitting, i.e. changes in PDFs relatively small, mainly in $d_V(x, Q^2)$.

Little tension with previous data – at NLO $\Delta\chi^2 = 9$ for the remainder of the data and at NNLO $\Delta\chi^2 = 8$.

Some reduction in details of flavour decomposition uncertainties, e.g. low- x valence quarks.

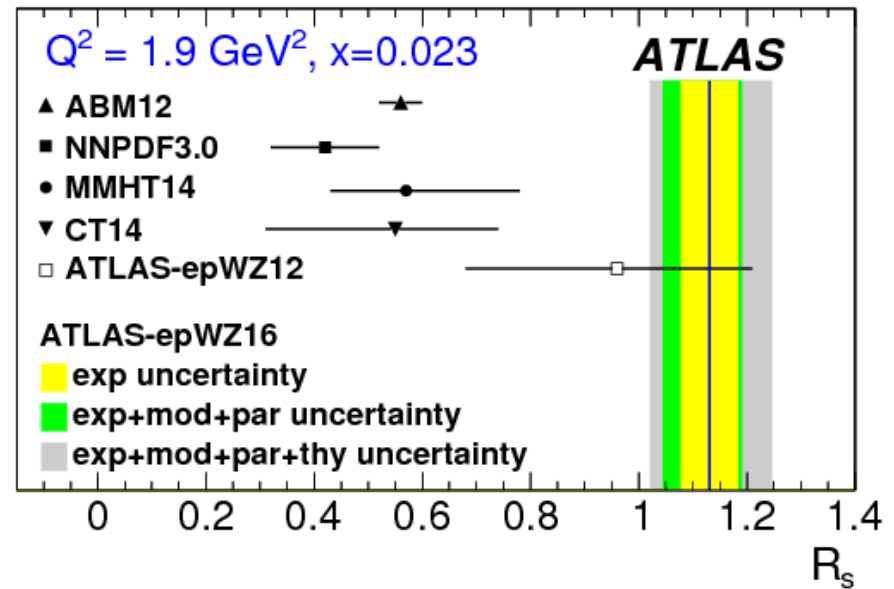
Extremely high precision data on W, Z from **ATLAS**



Difficulties in fitting both W and Z distributions fixed by increase in strange quark fraction

$$R_S = \frac{s + \bar{s}}{\bar{u} + d}$$

in **ATLAS** study.

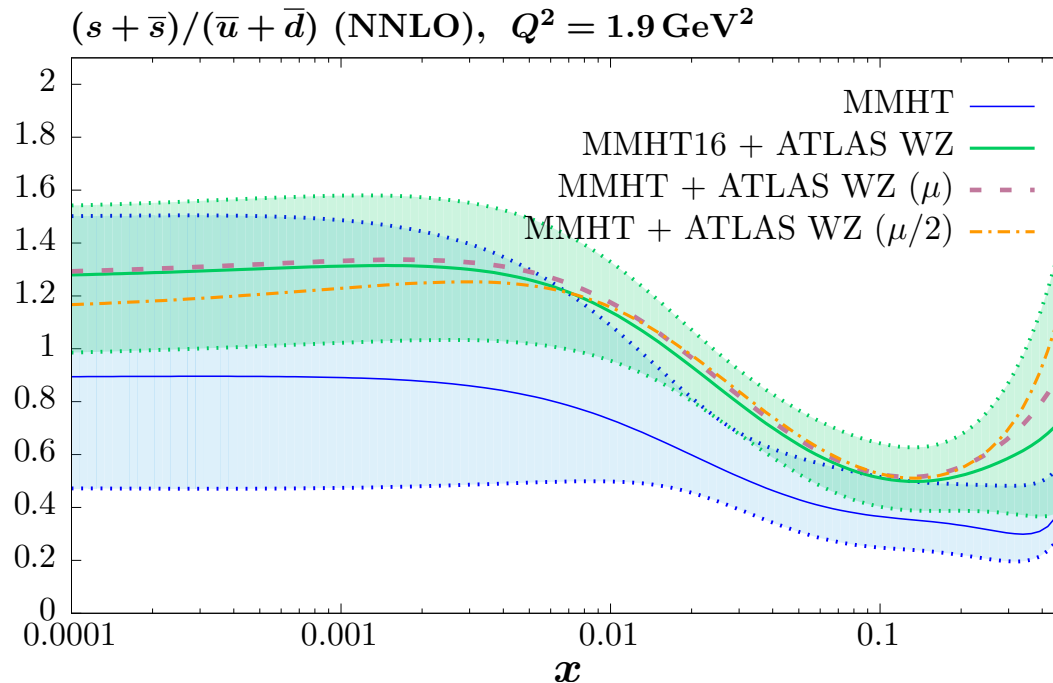


MMHT – updated fits also with high precision **ATLAS W, Z** data.

Including **ATLAS W, Z** data in fit goes from $\chi^2/N_{pts} \sim 387/61 \rightarrow \chi^2/N_{pts} \sim 108/61$ (scales set to $\mu_{R,F} = M_{W,Z}/2$).

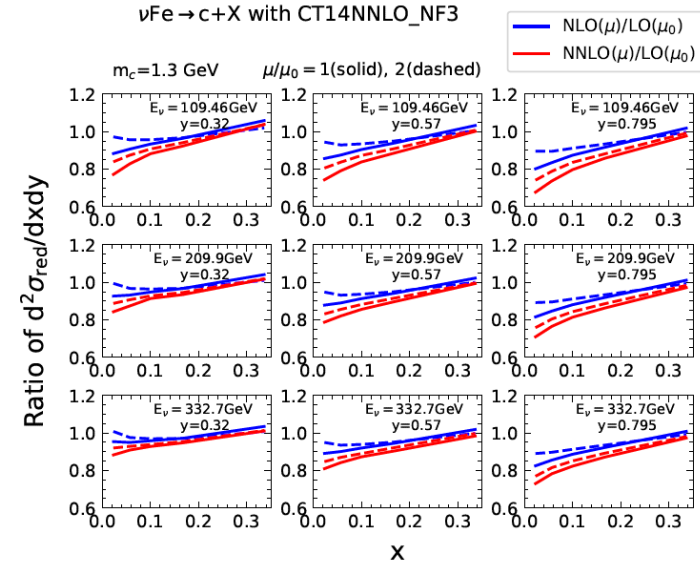
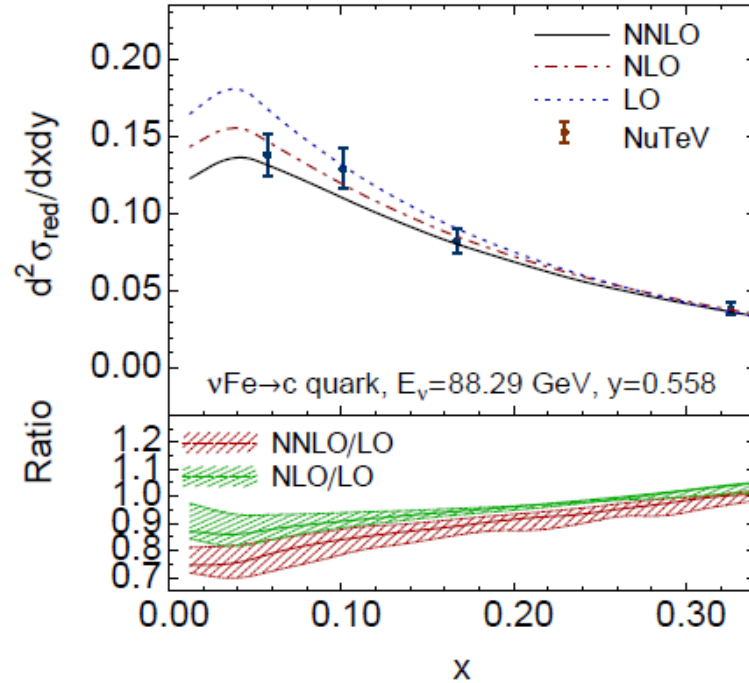
Deterioration in fit to other data $\Delta\chi^2 \sim 54$.

Mainly **CMS** $d^2\sigma/dMdy$ Z/γ , **CCFR/NuTeV** dimuon and **E866** DY asymmetry data.



At $x = 0.023$ $R_s \sim 0.83 \pm 0.15$. Compare to **ATLAS** with $R_s = 1.13^{+0.08}_{-0.13}$.

Details of tension of W, Z data may be mitigated by NNLO corrections to dimuon production (Phys. Rev. Lett. 116 (2016), Berger *et al.*, J. Gao, arXiv:1710.04258).



NNLO correction negative, but larger in size at lower x

Now include these in fit (**Bailey**) (required some improvement in threshold treatment for charged-current **VFNS** scheme).

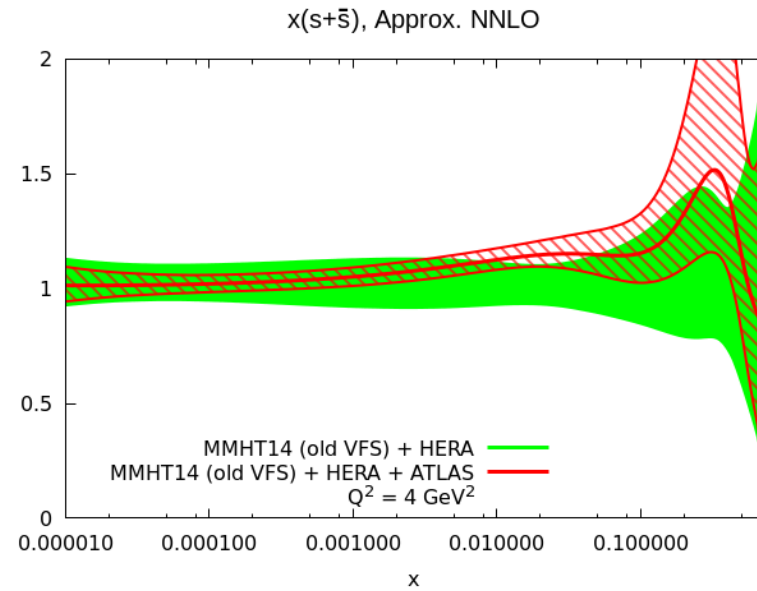
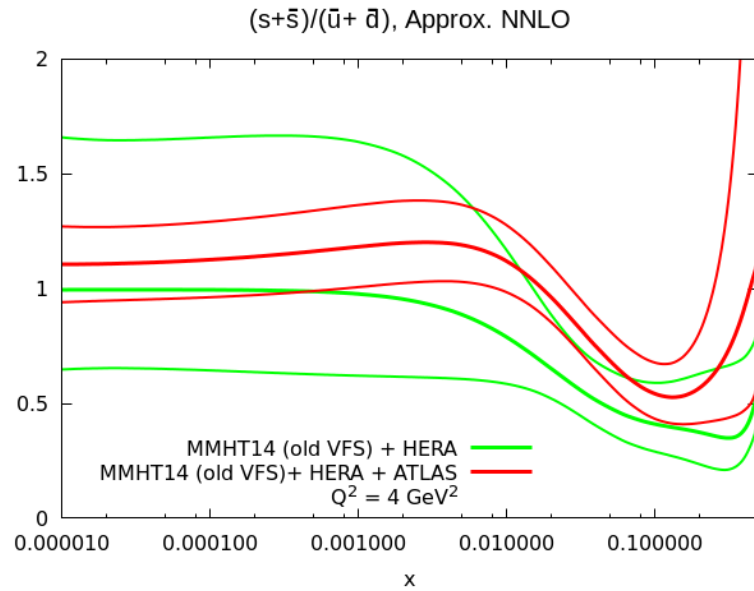
	$\text{BR}(c \rightarrow \mu)$	CCFR/NuTeV χ^2	ATLAS $W, Z \chi^2$	Total χ^2
MMHT+HERAII	0.090	120.5		3526.3
MMHT+HERAII (NNLO dimuon)	0.102	122.7		3527.3
MMHT+HERAII (NNLO VFNS dimuon)	0.101	123.9		3531.3
MMHT+HERAII+ATLAS(W, Z)	0.073	127.3	108.6	3684.7
MMHT+HERAII+ATLAS(W, Z) (NNLO dimuon)	0.084	137.8	106.8	3688.4
MMHT+HERAII+ATLAS(W, Z) (NNLO VFNS dimuon)	0.086	137.0	106.8	3688.5
N_{pts}		126.25	61	3337

The default value of $\text{BR}(c \rightarrow \mu) = 0.092 \pm 10\%$.

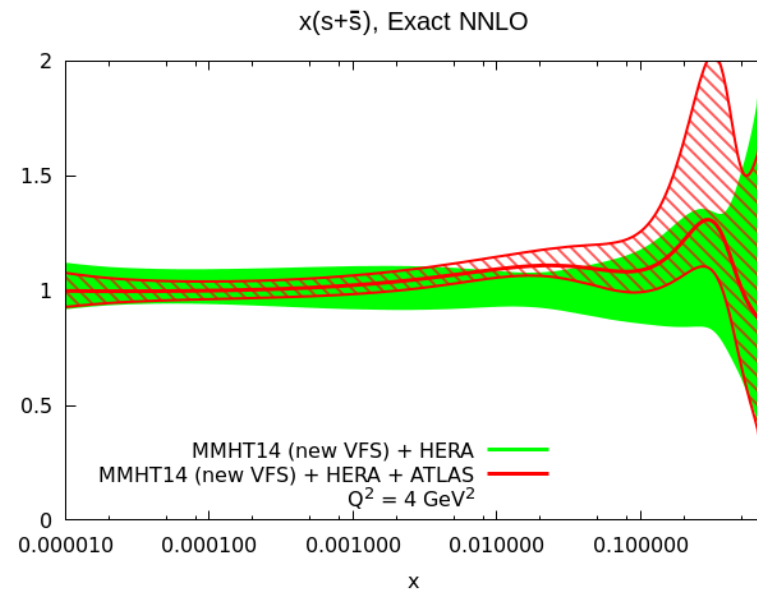
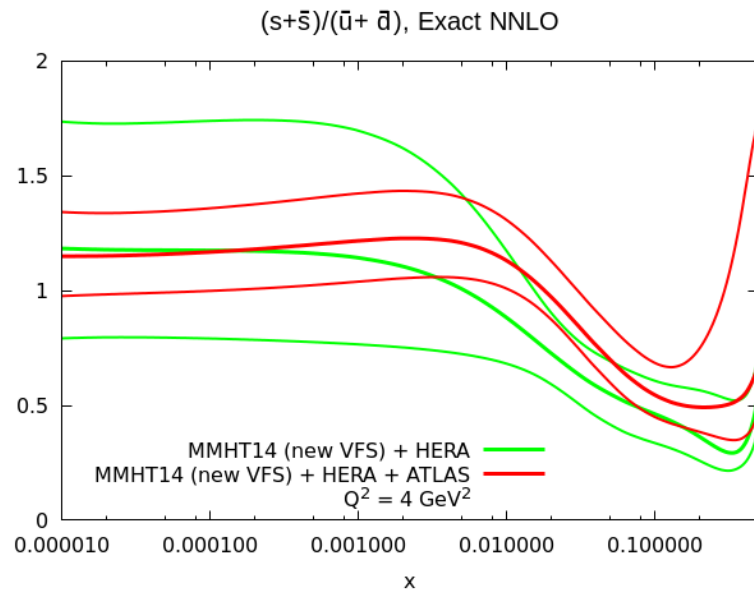
Also direct constraint on Strange from $W + c$ differential distributions.
CMS 7 TeV data in **MMHT** fit.

Newer **CMS** data at **13 TeV** – doesn't favour very large $s + \bar{s}$.

$s + \bar{s}$ illustration without full NNLO, i.e. as in MMHT2014.



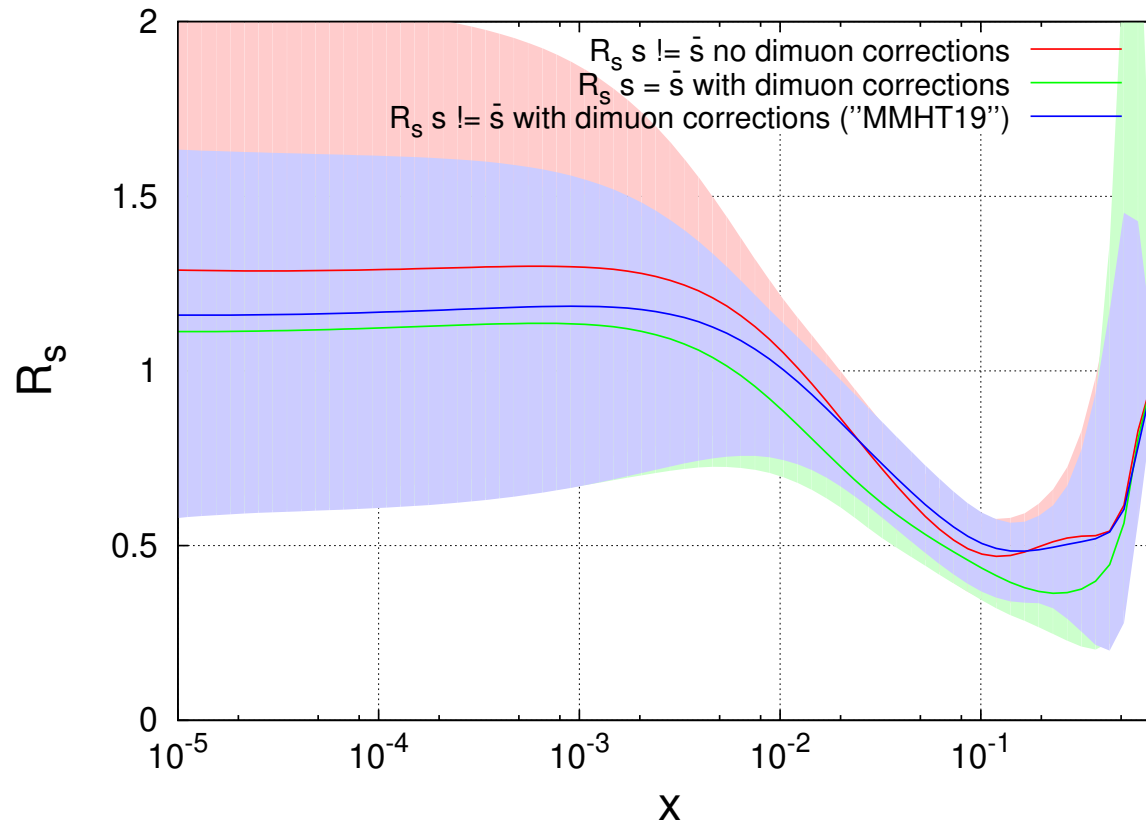
$s + \bar{s}$ illustration with full NNLO and updated VFNS.



Investigation of $s = \bar{s}$.

MMHT allow $s \neq \bar{s}$ in all fits. However, some other fits do not.

In particular ATLASepWZ16 PDF which sees $R_S = 1.13$. Could restriction be related to large R_S ?



$s = \bar{s}$ in MMHT leads to smaller R_S , but caused by best fit to dimuon data picking larger $\text{BR}(c \rightarrow \mu)$. No direct analogy to ATLAS study.

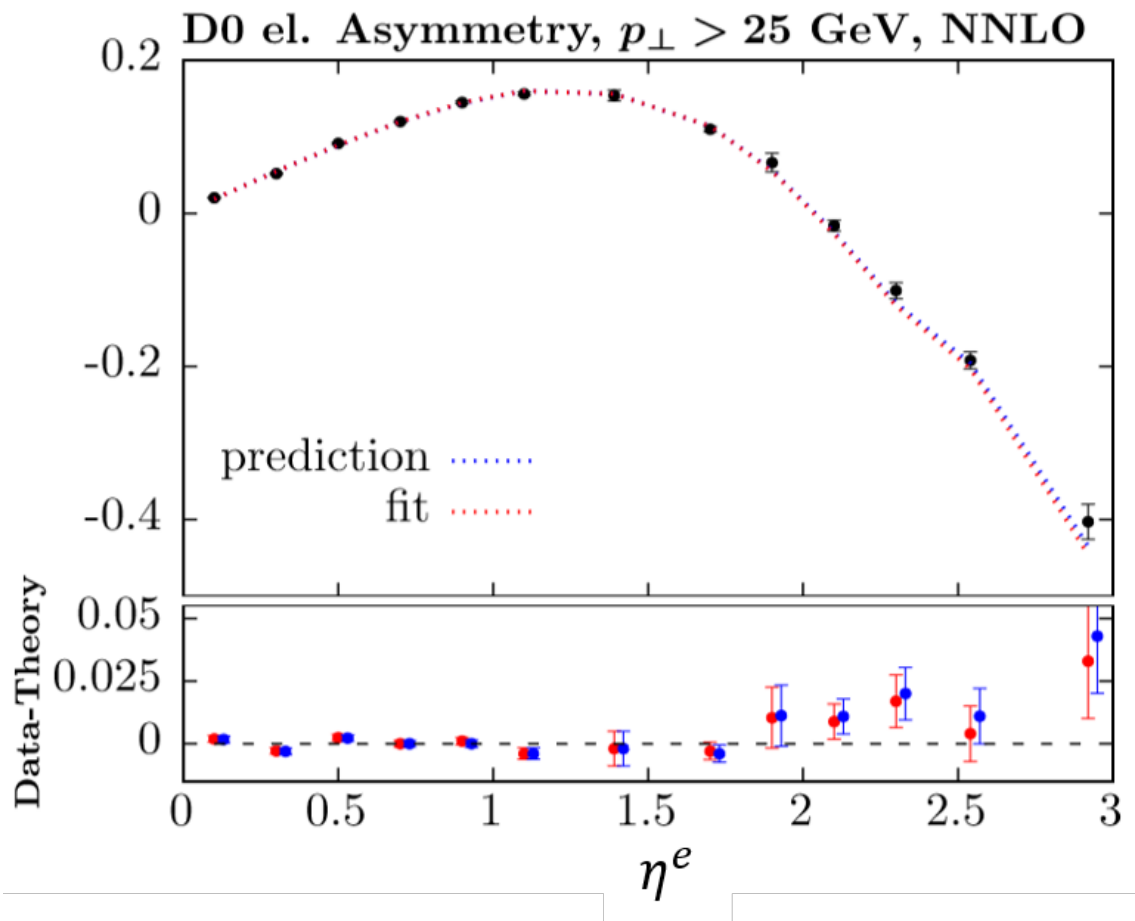
Additional new data sets - D0 electron/ W asymmetry

Already mentioned D0 e asymmetry [Phys. Rev. D 91, 032007 \(2015\)](#).

Good agreement with MMHT.

Slight undershoot at high η^e , implying smaller $d_v(x)$ not favoured by other data.

Can alternatively use W -asymmetry for same data [Phys. Rev. Lett. 112, 151803 \(2014\)](#).



$W^{+/-}$ produced preferentially in proton/antiproton direction.

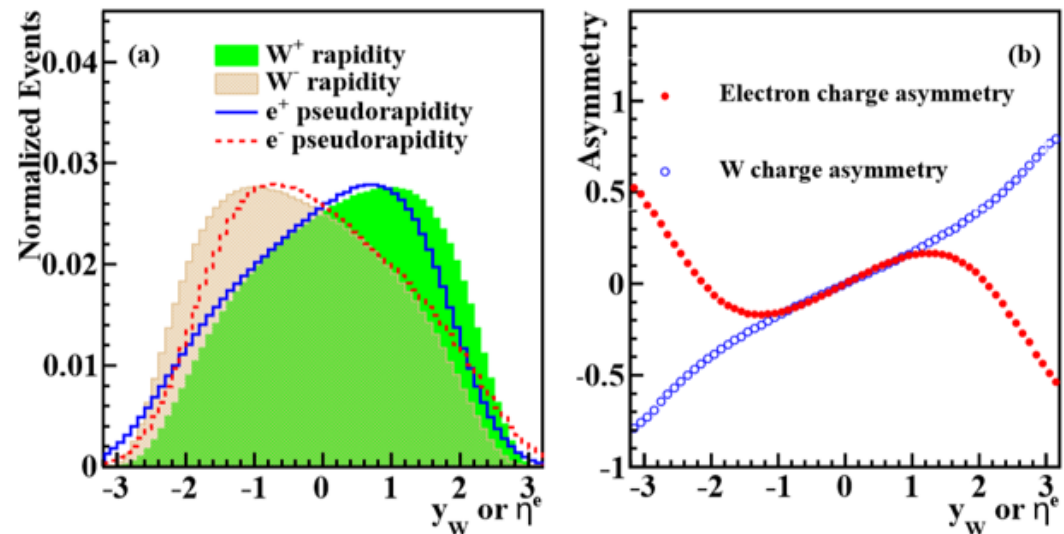
$V - A$ structure of lepton decay means $e^{+/-}$ emitted preferentially opposite to $W^{+/-}$.

Leptons at particular η^e come from range of η^W values and dilute direct constraint on PDFs at given x .

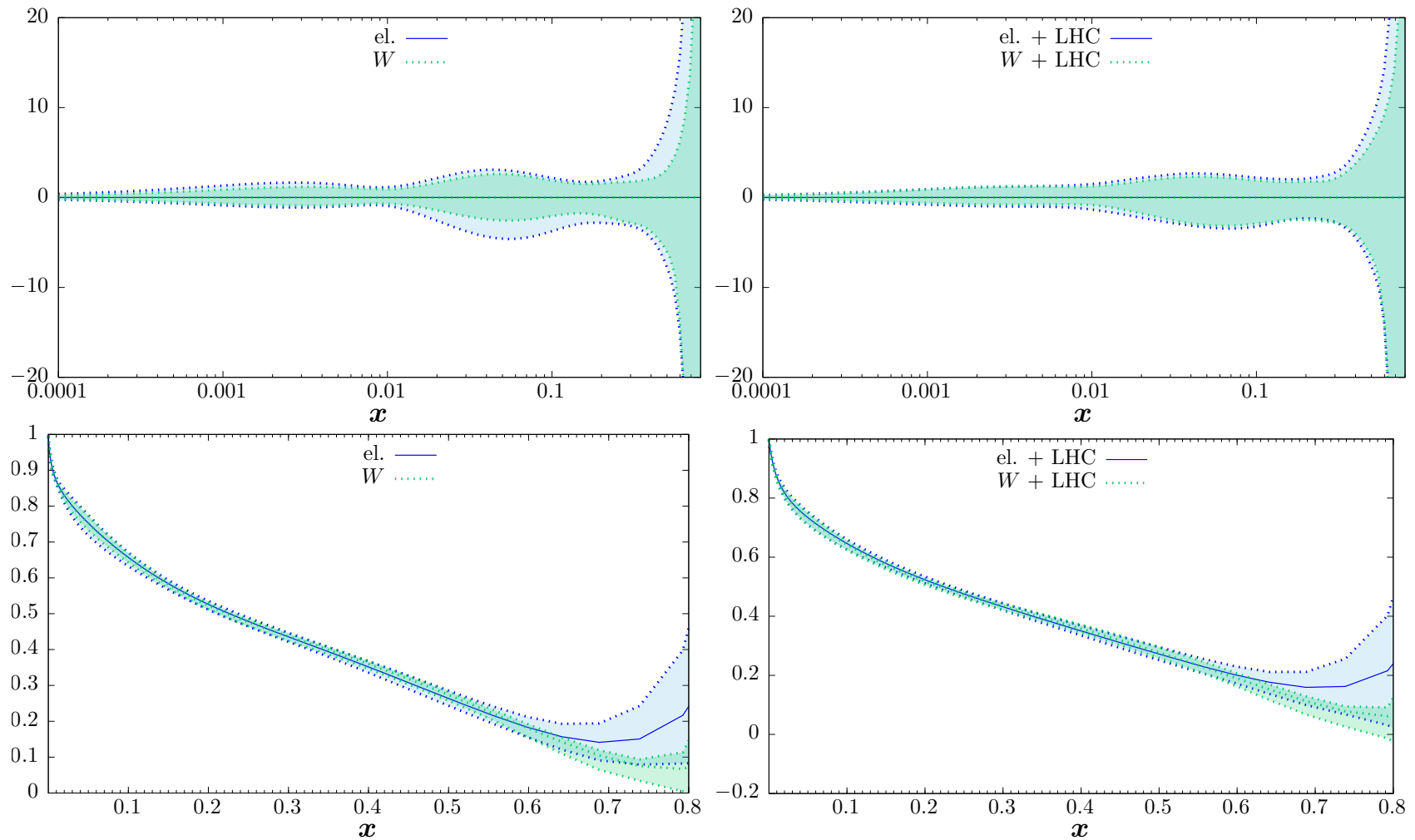
Mapping lepton asymmetry to W asymmetry requires PDF-dependent modelling with **small** uncertainty.

PDF induced uncertainty minor at high x compared to smearing effect in lepton uncertainty

Better constraint from W asymmetry.



See reduced uncertainty on d/u compared to e asymmetry, but less relative effect on top of LHC data.



Main effect at very high x , where d_v reduced.

Extension of parameterisation. (Cridge)

General parameterisation used $A(1-x)^\eta x^\delta (1 + \sum_{i=1}^n a_i T_i(1 - 2x^{\frac{1}{2}}))$, where $T_i(1 - 2x^{\frac{1}{2}})$ are Chebyshev polynomials.

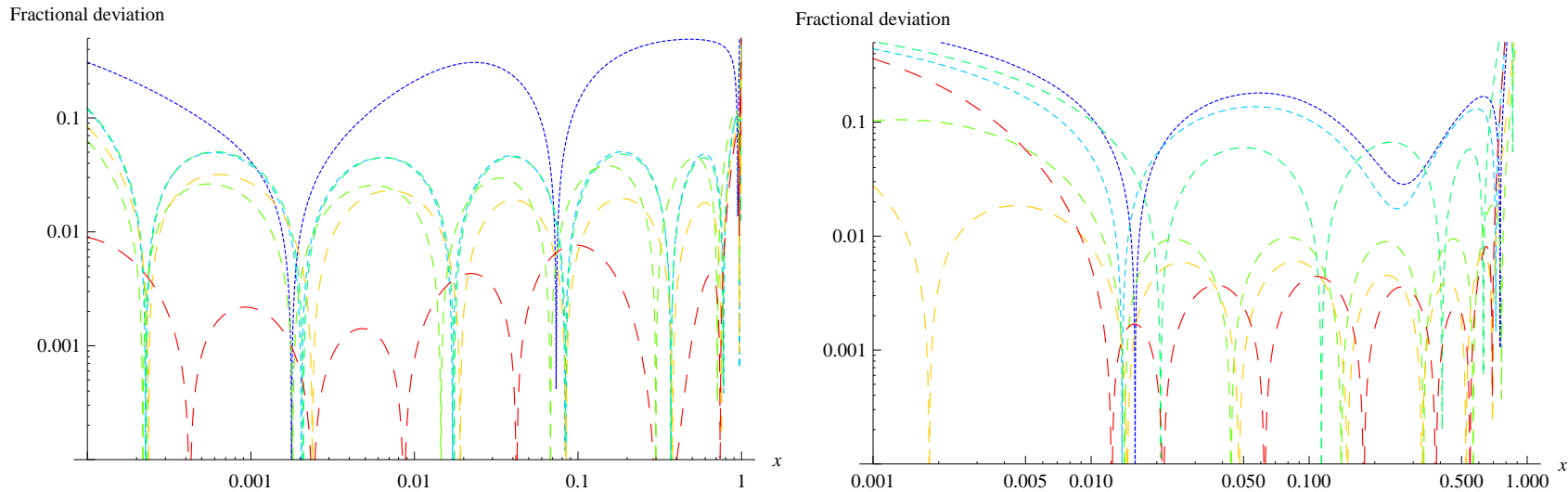


Illustration of precision possible with increasing n , sea-like (left) and valence-like (right) (where pseudo-data for $x > 0.01$). Using $n = 6$ would lead to much better than 1% precision.

For most PDFs $n = 4$ is default for **MMHT2014** - $g(x, Q_0^2)$ has a negative term, $s^+(x, Q_0^2)$ has two parameters tied to the sea and $(\bar{d} - \bar{u})(x, Q_0^2)$ and $s^-(x, Q_0^2)$ have fewer parameters. 36 parameters in total.

Try extending parameters of other PDFs sequentially using $n = 6$:

$$u_v(x, Q_0^2) = A_u(1-x)^{\eta_u} x^{\delta_u} (1 + \sum_{i=1}^6 a_{i,u} T_i(1-2x^{\frac{1}{2}})); A_u \text{ fixed by } \int_0^1 u_v dx = 2$$

$$d_v(x, Q_0^2) = A_d(1-x)^{\eta_d} x^{\delta_d} (1 + \sum_{i=1}^6 a_{i,d} T_i(1-2x^{\frac{1}{2}})); A_d \text{ fixed by } \int_0^1 d_v dx = 1$$

$$sea(x, Q_0^2) = A_S(1-x)^{\eta_S} x^{\delta_S} (1 + \sum_{i=1}^6 a_{i,S} T_i(1-2x^{\frac{1}{2}}));$$

$$s^+(x, Q_0^2) = A_s(1-x)^{\eta_s} x^{\delta_s} (1 + \sum_{i=1}^6 a_{i,s} T_i(1-2x^{\frac{1}{2}})); a_{i,s} = a_{i,S}, i = 5, 6$$

$$(\bar{d} - \bar{u})(x, Q_0^2) = A_{\Delta}(1-x)^{\eta_{\Delta}} x^{\delta_{\Delta}} (1 + \sum_{i=1}^6 a_{i,\Delta} T_i(1-2x^{\frac{1}{2}}));$$

$$g(x, Q_0^2) = A_g(1-x)^{\eta_g} x^{\delta_g} (1 + \sum_{i=1}^4 a_{i,g} T_i(1-2x^{\frac{1}{2}})) - A_{g-}(1-x)^{\eta_{g-}} x^{\delta_{g-}};$$

$$s^-(x, Q_0^2) = A_{s-}(1-x)^{\eta_{s-}} (1-x_o/x) x^{\delta_{s-}}. x_o \text{ fixed by } \int_0^1 s^- dx = 0, \delta_{s-} \text{ fixed.}$$

Change of to a maximum of 51 parton parameters.

Improvements in Global Fit.

Main improvements after extension of $(\bar{d} - \bar{u})(x, Q_0^2)$ from additionally introducing $d_V(x, Q_0^2)$ ($u_V(x, Q_0^2)$ not significant) and $g(x, Q_0^2)$ ($sea(x, Q_0^2)$ and $s^+(x, Q_0^2)$ not significant).

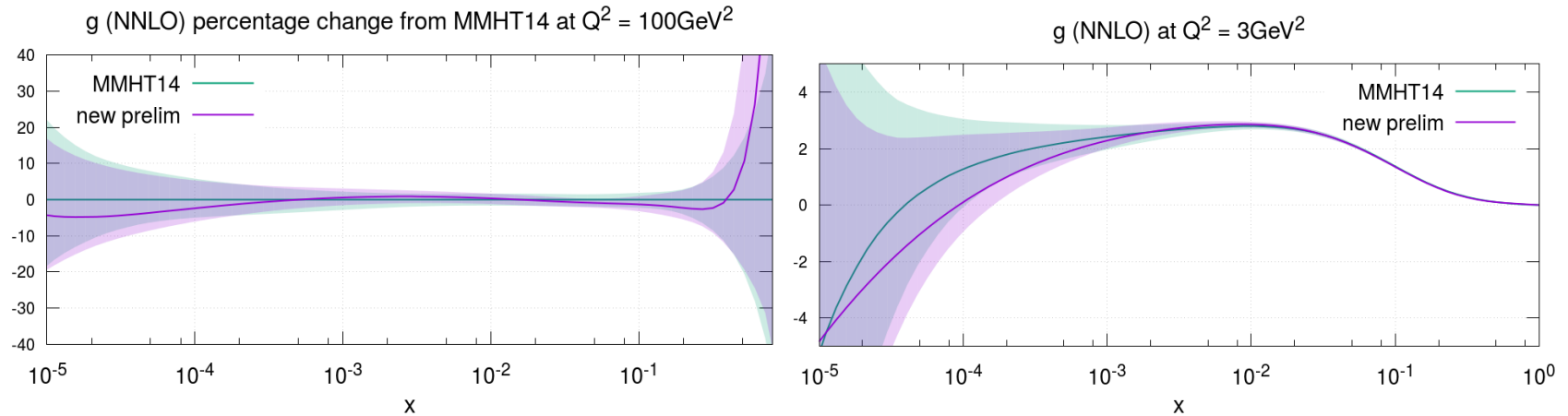
Data set	$-\Delta\chi^2$ $(\bar{d} - \bar{u})$	$-\Delta\chi^2$ $(\bar{d} - \bar{u}), d_v$	$-\Delta\chi^2$ All
Total	17.6	34.0	48.9
BCDMS F_2^p	-4.6	-3.3	-2.7
BCDMS F_2^d	-2.7	4.9	8.5
NMC F_2^n / F_2^p	6.5	6.1	6.0
NuTeV F_3^N	-0.3	1.7	3.2
E866 $\sigma(pd) / \sigma(pp)$	8.2	10.1	11.0
NuTeV dimuon	0.7	1.0	3.0
HERA I+II $\sigma(e^+p)$ 920 GeV	1.1	1.7	4.6
CMS $pp \rightarrow l^+l^-$	0.7	1.8	3.1
D0 $\sigma(e^+) - \sigma(e^-)$	-1.2	-3.4	-1.4
CMS 8 TeV $\sigma(l^+) - \sigma(l^-)$	4.4	5.0	4.6
ATLAS 7 TeV W, Z	-0.5	2.2	4.3
CMS 7 TeV jets	-0.5	0.2	3.2

Reduces tension between **DY ratio** data and **LHC** data, rather than improving intrinsic fit quality to **DY ratio** (**MMHT** fit nearly optimal).

LHC lepton asymmetry improved, but **D0** worse.

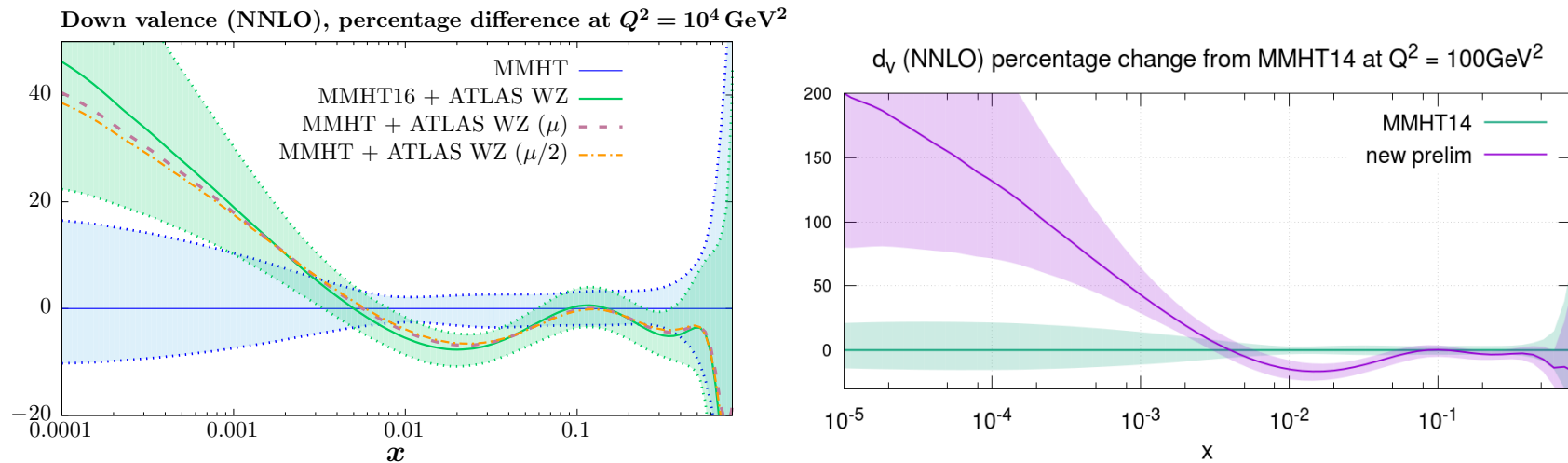
Gluon-induced improvement only partially from **HERA** data.

Plots of $g(x, Q^2)$ at high and lower Q^2 .



Some features in common with change in [arXiv:1902.11125](#), but initial parameterisation much more free here.

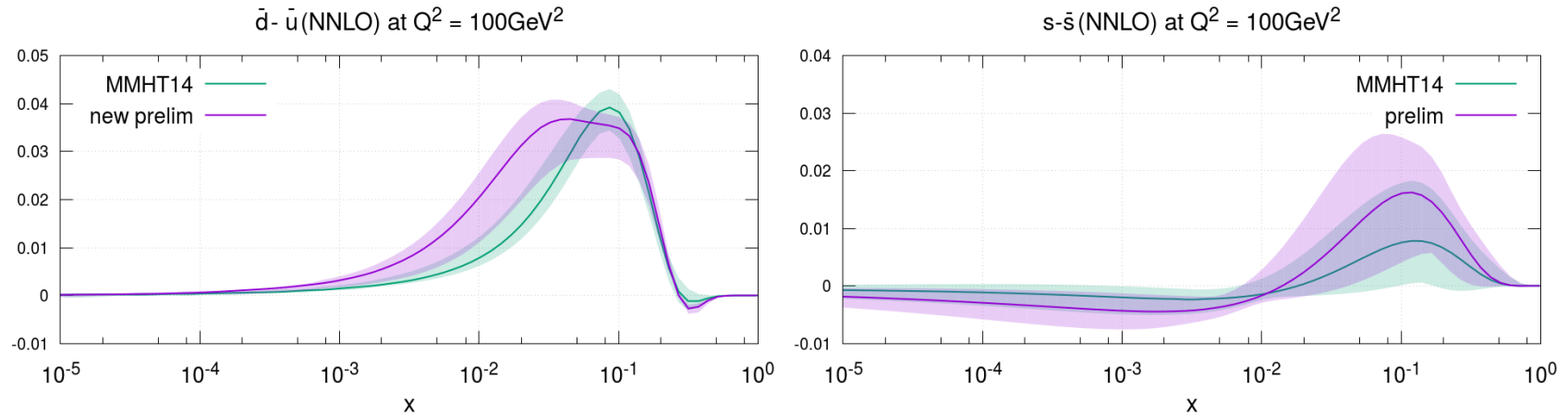
The biggest change is in $d_V(x, Q^2)$ - largely due to 7 TeV ATLAS W, Z data, and extra parameterisation has a significant effect.



Left – new data. Right – new data and extended parameterisation.

Note increased uncertainty at very large and small x due to extended parameterisation. Former a feature of many PDFs.

Plots of $(\bar{d} - \bar{u})(x, Q^2)$ and $(s - \bar{s})(x, Q^2)$



Increase in size of $(s - \bar{s})(x, Q^2)$ driven by data – overwhelmingly 7 TeV ATLAS W, Z data. No change in parameterisation.

Data prefer a distinctly different shape in $(\bar{d} - \bar{u})(x, Q^2)$ and extra parameter gives extra uncertainty (just about goes negative in places).

However, error bands for $(\bar{d} - \bar{u})(x, Q^2)$ still shrink $\rightarrow 0$ as $x \rightarrow 0$ due to parameterisation.

Try $\rho(x, Q_0^2) \equiv \frac{\bar{d}}{\bar{u}}(x, Q_0^2) = A_\Delta(1-x)^{\eta_\Delta}(1 + \sum_{i=1}^6 a_{i,\delta} T_i(1 - 2x^{\frac{1}{2}}))$;

$\rho(x, Q_0^2) \rightarrow$ (free) constant as $x \rightarrow 0$. Further improvement in fit quality, and much smaller Chebyshev coefficients. Now 50 free parameters.

Dataset	$-\Delta\chi^2(\bar{d} - \bar{u} \text{ 6 Chebyshevs})$	$-\Delta\chi^2(\bar{d}/\bar{u} \text{ 6 Chebyshevs})$
Total	48.9	55.2
BCDMS	5.8	3.0
NMC F_2^n/F_2^p	5.1	6.1
NuTeV F_3^N	3.2	2.5
E866 DY ratio $\sigma(pd)/\sigma(pp)$	11.0	10.1
NuTeV dimuon	3.0	-0.3
Hera CC $\sigma(e^+p)$	0.6	5.7
Hera CC $\sigma(e^-p)$	-0.2	-3.7
Hera I+II $\sigma(e^+p)$ NC	4.2	6.4
Hera I+II $\sigma(e^-p)$ NC	-2.1	1.9
D0 $\sigma(e^+) - \sigma(e^-)$ old+new	0.1	-2.4
D0 $\sigma(\mu^+) - \sigma(\mu^-)$	-1.4	-2.9
CDF W asymmetry	1.7	4.0
LHCb 7 TeV W+Z	-0.3	1.6
LHCb 7+8TeV W,Z muon	-2.5	-5.1
CMS Neutral current(Z/γ) DY	3.1	10.0
CMS 8TeV W $\sigma(l^+) - \sigma(l^-)$	4.6	0.5
ATLAS 7TeV W,Z	4.3	4.8
CMS 7 TeV jets	3.2	4.9

When determining uncertainties go from 25 eigenvector pairs to 30 - one extra parameter for each PDF other than for the light sea and $s^-(x, Q_0^2)$.

Mean tolerance $T = 3.47$

29 eigenvector directions constrained primarily by LHC data sets – largely 7 TeV ATLAS W, Z data and CMS W (and $W + c$) data but some others including LHCb top and jets.

8 eigenvectors — E866 Drell Yan asymmetry vital for constraining $\bar{d} - \bar{u}$.

8 eigenvectors – Tevatron data of various types primary constraint.

10 eigenvectors – fixed target DIS data (BCDMS, NMC, NuTeV, CCFR) still constrains mainly high- x .

Fully global fit necessary for full constraint with (almost) no assumptions/models.

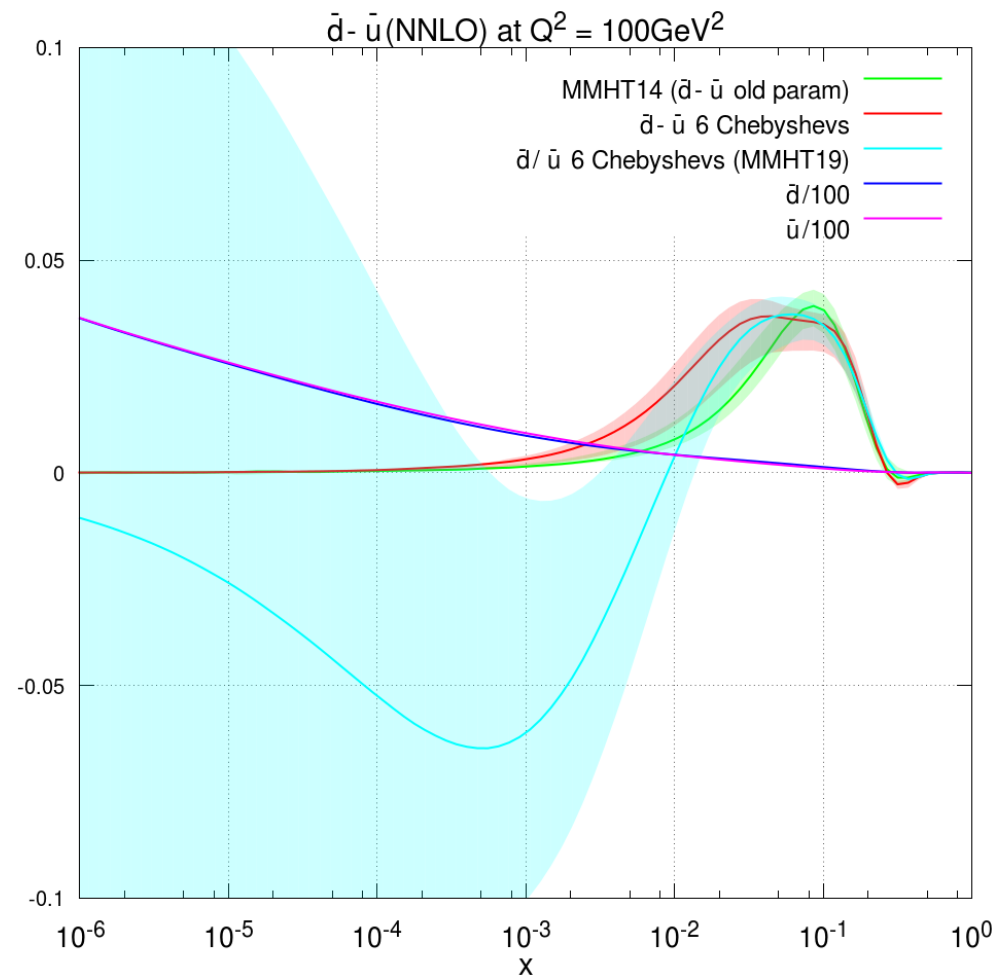
Parameterising as ratio
allows much larger relative
uncertainty at small x .

Note asymmetry much
smaller than \bar{d}, \bar{u} .

Also allows more complex
shape in this region.

$\bar{d} - \bar{u}$ turns negative at
small x with, at most,
 $\sim 1\sigma$ significance.

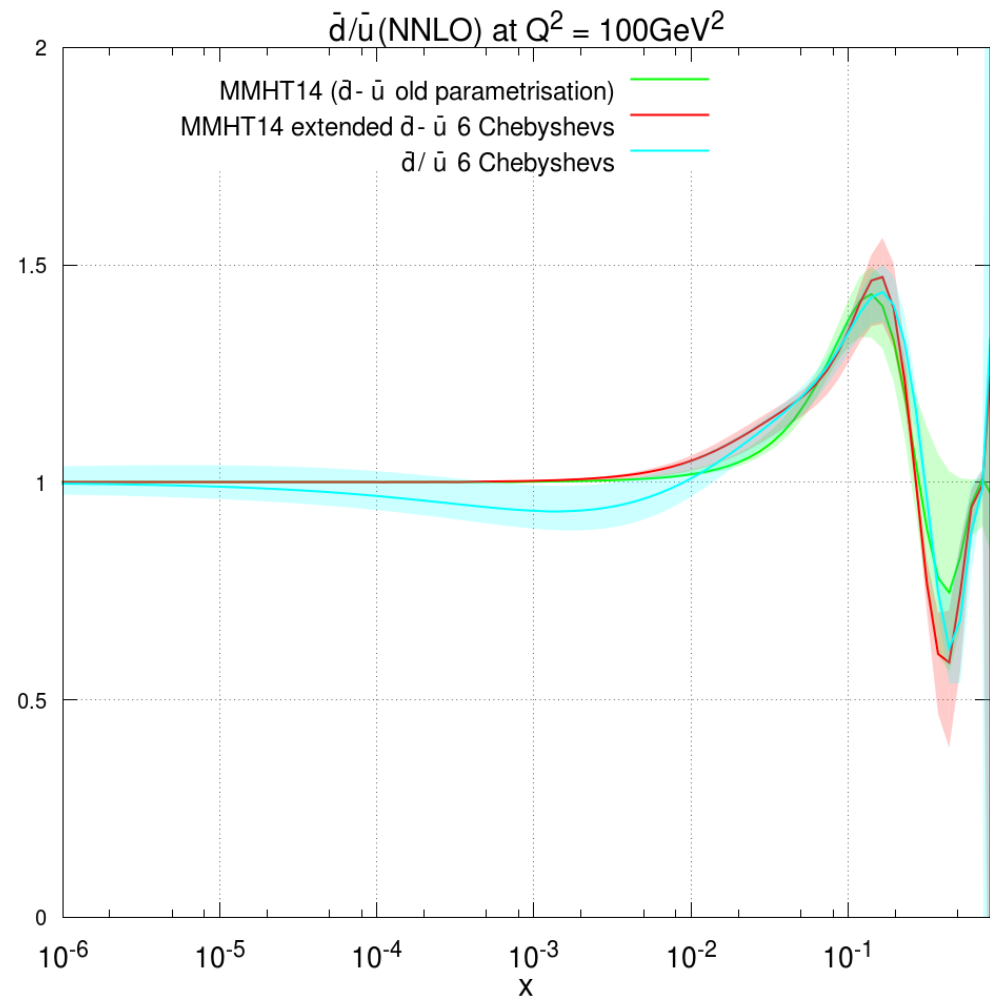
very similar to the
previous **MMHT** results
for $x > 0.01$ and within
 $\sim 1\sigma$ at small x .



Without being fixed \bar{d}/\bar{u} approaches a value close to unity as $x \rightarrow 0$ with few percent uncertainty.

Data constraint vanishes at very small x , but ratio has effectively reached constant for $x < 0.0001$.

Relatively weak pull to $\bar{d}/\bar{u} < 1$ at high x from E866 data.



Inclusion of final HERA $\tilde{\sigma}^{c\bar{c}}$ and $\tilde{\sigma}^{b\bar{b}}$ data **Eur.Phys.J.C78 (2018), 473.**

Fit fully up-to-date, except for Z p_T and $W + \text{jets}$ data.

Best fit $\chi^2 = 132/80$ for 52 $\tilde{\sigma}^{c\bar{c}}$ and 28 $\tilde{\sigma}^{b\bar{b}}$. (Correlations, both systematic and statistical, between data sets.)

No tension with other data within global fit, refit leads to very marginal improvement. Inclusive HERA data carries enormously more weight on relevant PDFs.

Though fit at low Q^2 not optimal, result seems similar to quality for other PDFs **Eur.Phys.J.C78 (2018), 473**, e.g.

- $\chi^2 = 102/52 + 45/28 = 147$ HERAPDF20–NNLO–EIG (RTOPT)
- $\chi^2 = 86/52 + 33/28 = 119$ HERAPDF20–NNLO–FF3A (FFNS)
- $\chi^2 = 109/52 + 41/28 = 150$ ABMP16–3–nnlo (FFNS)

where the two data types have been fit independently so a direct comparison is not possible.

Variation with m_c (for free $\alpha_s(M_Z^2)$) at NNLO.

m_c (GeV)	χ^2_{global} 3793 pts	$\chi^2_{\tilde{\sigma}^{c\bar{c}}+\tilde{\sigma}^{b\bar{b}}}$ 80 pts	$\alpha_s(M_Z^2)$
1.3	4218	140	0.1171
1.35	4215	135	0.1172
1.4	4215	132	0.1174
1.45	4216	133	0.1173
1.5	4221	134	0.1174

Unlike our previous results (Eur.Phys.J. C76 (2016)) which preferred lower values ($m_c^{\text{pole}} \sim 1.25\text{GeV}$), default choice of $m_c^{\text{pole}} = 1.4\text{GeV}$ seems about optimal.

No improvement from variation in assumptions about $\mathcal{O}(\alpha_s^3)$ FFNS coefficient functions at low Q^2 .

Very weak preference for slight increase in default $m_b^{\text{pole}} = 4.75\text{GeV}$ for $\tilde{\sigma}^{b\bar{b}}$ and slight decrease for global fit.

Inclusion of LHC data on $W + \text{jets}$ p_T distribution. (Cridge)

8 TeV ATLAS $W^+ + \text{jets}$ and $W^- + \text{jets}$ data (JHEP 05 (2018) 077) fit as a function of p_T^W .

Sensitive to the gluon and u and d quarks and antiquarks, particularly at high x .

Apply NNLO K -factors (Phys. Rev. Lett. 115 (2015) 062022) and non-perturbative corrections obtained using SHERPA.

Former consistently $\sim 10\%$ and latter very small except first bin, $p_T^W < 25 \text{ GeV}$, where both $> 20\%$. Resummation effects also expected to be large here.

Fit within MMHT2019 framework.

	Including First p_T^W bin	Not Including First p_T^W bin
Not refit	40.1 / 32	20.4 / 30
Refit	39.9 / 32	20.1 / 30

Clear issue with first p_T^W bin.

Compare with [ATLASepWZ19U+ \$p_T^W\$](#) which report $\chi^2 = 18/34$ (including first bin) plus penalty from correlated uncertainty.

We obtain $\chi^2 = 39.9/32$ of which 19.7 is χ^2 penalty, so similar.

Excluding first bin gives total $\chi^2 = 20.1$ and penalty is 7.6

Even including first bin, data already fit very well, very marginal improvement on refitting.

Consistent with other data. Very small tension with [HERA](#) data and [CMS](#) lepton rapidity data, pulls in same direction as most [LHC](#) data.

Inclusion of LHC data on Z p_T distribution - preliminary.

Include 8 TeV CMS data on $d\sigma/dp_T^{ll}$ in rapidity bins for invariant mass near Z peak (Phys.Lett. B749 (2015) 187), and 8 TeV ATLAS data (Eur.Phys.J. C76 (2016) 291) in rapidity bins for invariant mass near Z peak, and inclusive in rapidity for low and high mass bins.

Cut for $p_T > 30\text{GeV}$. Include high p_T , and will add electroweak corrections in future (not a big effect).

Like NNPDF, Eur.Phys.J. C77 (2017) 663 find problems with highest rapidity bin for CMS data.

Adding to MMHT14 framework find $\chi_{\text{ATLAS}}^2 \sim 136/80$ and $\chi_{\text{CMS}}^2 \sim 43/32$.

Fairly similar to NNPDF, but we use smooth fit K -factors (with uncertainty) for NNLO correction, rather than $\sim 1\%$ point-by-point theoretical uncertainty (as with jets).

Main effect – pulls $\alpha_S(M_Z^2)$ in fit up by 0.001 – similar to effect seen by NNPDF, Eur.Phys.J. C78 (2018) 408. No obvious data tensions except as consequence of increased $\alpha_S(M_Z^2)$ (e.g BCDMS).

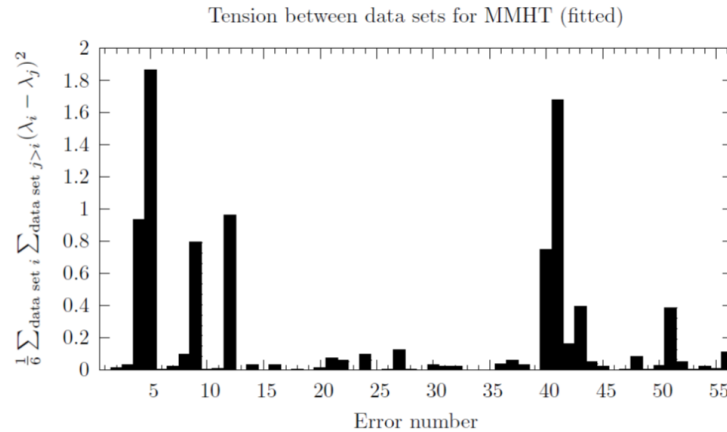
Differential $t\bar{t}$ data. Bailey

A similar issue noticed in differential top-antitop production [ATL-PHYS-PUB-2018-017](#) - NNLO now available [Czakon et al](#)).

Distributions differential in $y_t, y_{\bar{t}}, p_T^t, M_{t\bar{t}}$, and statistical correlations available (not fully implemented yet).

Find similar issues with correlated uncertainties when fitting all together, and fitting $y_t, y_{\bar{t}}$ individually (seen by [MMHT](#), [CT](#), [ATLAS](#) not [NNPDF](#).)

		Fitted data set(s)				
		p_T	y_t	$y_{\bar{t}}$	$M_{t\bar{t}}$	All
Contribution	p_T	0.08				2.38
	y_t		1.23			1.84
	$y_{\bar{t}}$			1.09		2.22
	$M_{t\bar{t}}$				0.29	1.81
	Penalty	0.24	1.83	2.35	0.17	0.88
	Total	0.32	3.06	3.44	0.47	2.96

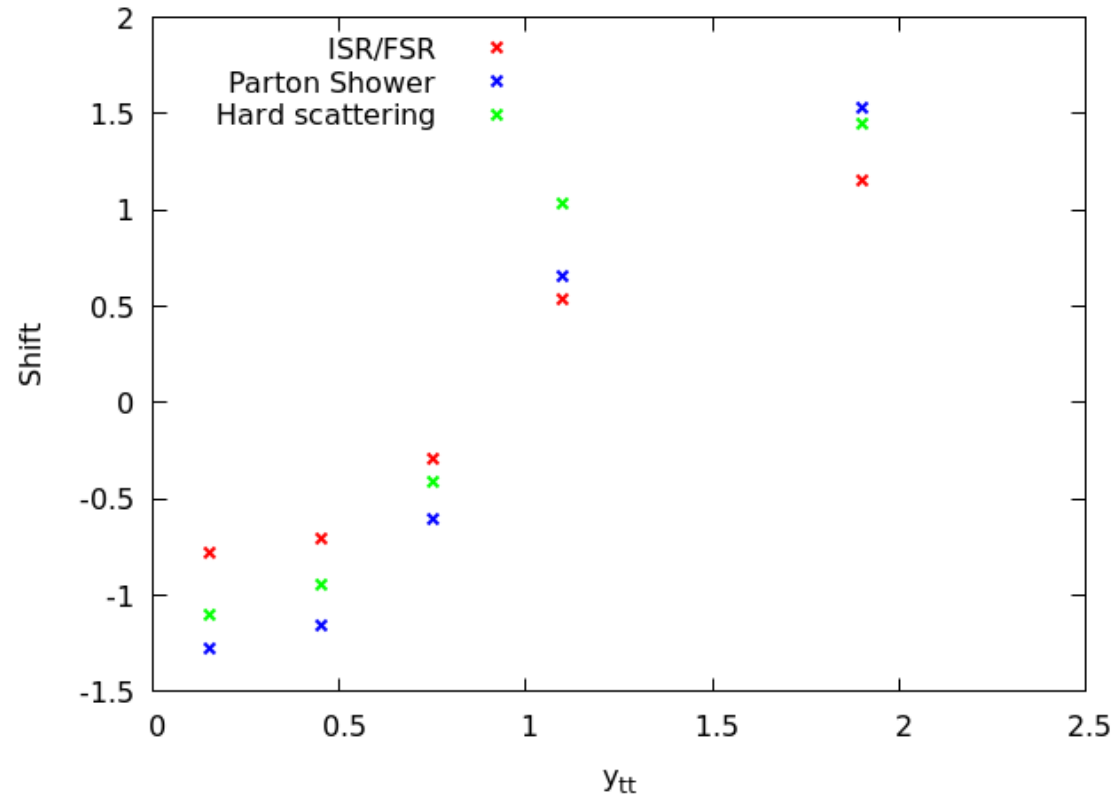


χ^2/N high in simultaneous fit and for rapidity distributions.

Highly sensitive to correlations in 3 large systematics – hard-scattering model, ISR/FSR and parton Shower. All Monte Carlo related.

$y_{\bar{t}t}, y_t$ fits still poor when decorrelating between types of distribution only.

For $y_{\bar{t}t}$ desired shift varies considerably between points.



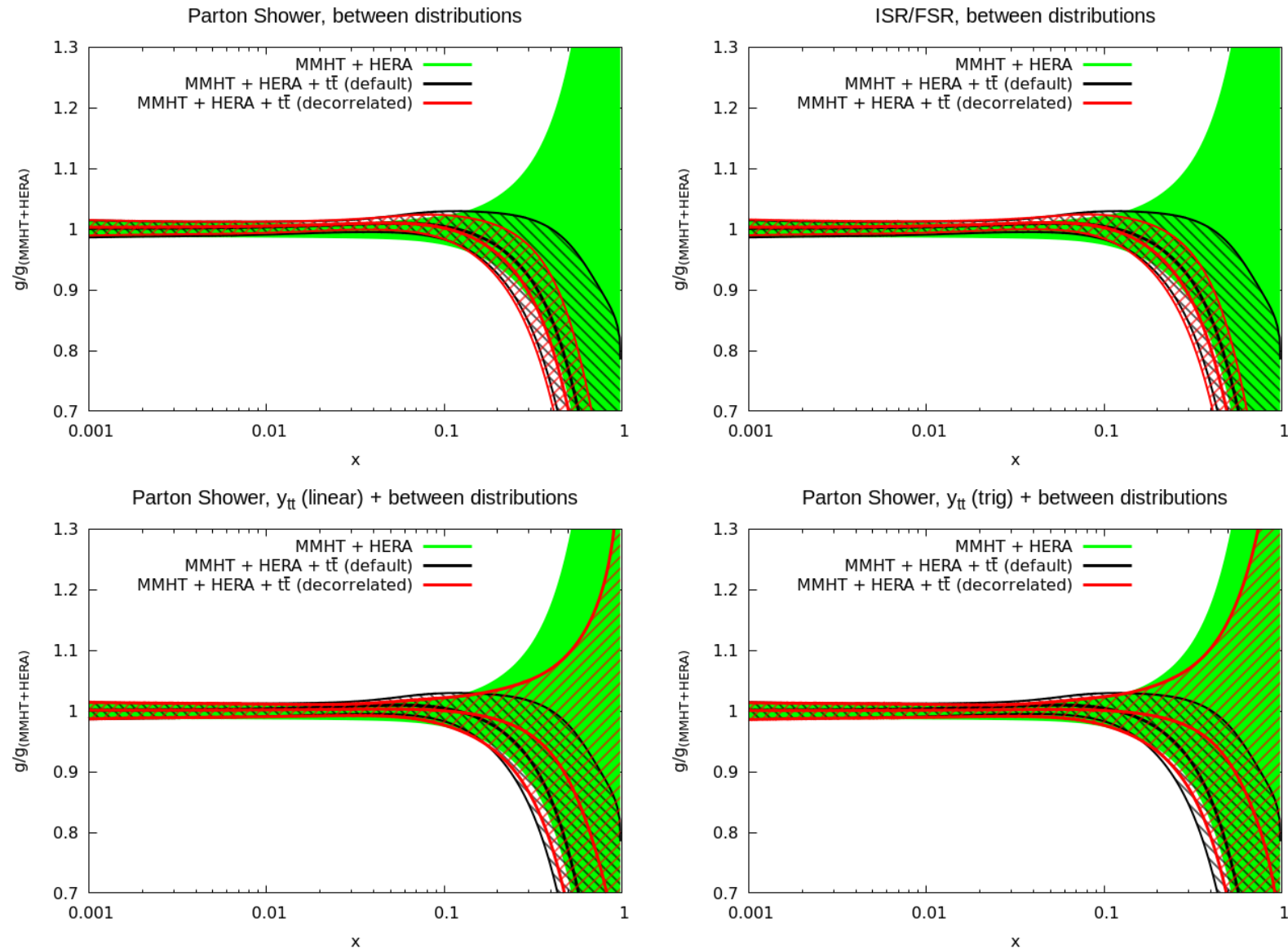
Try decorrelating for individual distribution and between sets.

Two types of decorrelation for parton shower.

$$\beta_i^1 = \left(\frac{y_{tt,i} - y_{tt,min}}{y_{tt,max} - y_{tt,min}} \right) \beta_i^{\text{tot}}, \quad \beta_i^2 = \left[1 - \left(\frac{y_{tt,i} - y_{tt,min}}{y_{tt,max} - y_{tt,min}} \right) \right]^{\frac{1}{2}} \beta_i^{\text{tot}} \quad \beta_i^1 = \cos \left[\pi \left(\frac{y_{tt,i} - y_{tt,min}}{y_{tt,max} - y_{tt,min}} \right) \right] \beta_i^{\text{tot}}, \quad \beta_i^2 = \sin \left[\pi \left(\frac{y_{tt,i} - y_{tt,min}}{y_{tt,max} - y_{tt,min}} \right) \right] \beta_i^{\text{tot}}$$

Sine-cosine decorrelation works better.

Results on the gluon moderately independent of decorrelation and method.



Perhaps better justification for decorrelation than for than jets.

MMHT PDFs with QED corrections – Nathvani (Eur. Phys. Jour. C)

Base photon input for PDFs at $Q_0^2 = 1\text{GeV}^2$ on LUX – much better constraint than previously.

Input defined by integrating LUX expression up to scale $\mu^2 = Q_0^2$. Input momentum for photon = 0.00195.

Effect of photon evolution fully incorporated to couple with that of quarks and gluon for both proton and neutron.

PDFs evolve up using DGLAP splitting functions to given order in α_s with α , $\alpha\alpha_s$ and α^2 corrections (De Florian *et al*) included.

In addition the photon receives contributions/corrections from “higher twist” sources above $Q_0^2 = 1\text{GeV}^2$ – elastic, target mass, kinematic cuts, higher twist (renormalon) corrections to $F_2(x, Q^2)$. Tiny ($\mathcal{O}(10^{-4})$) momentum violation.

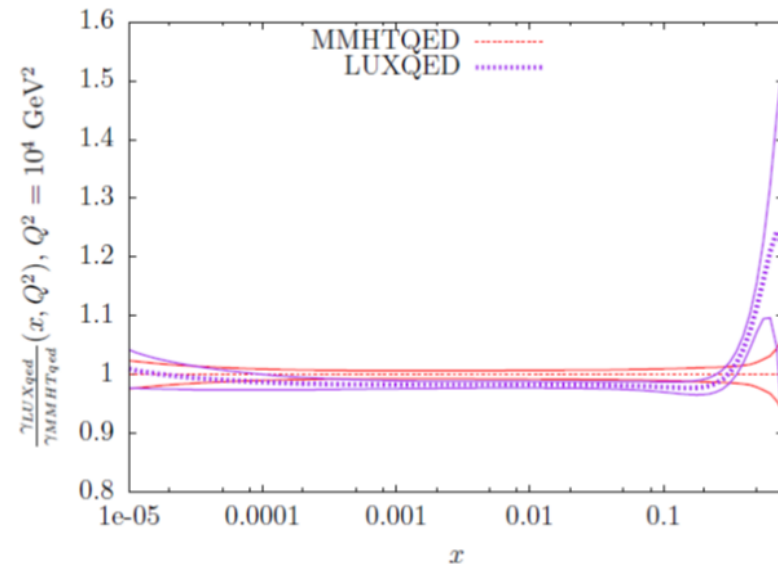
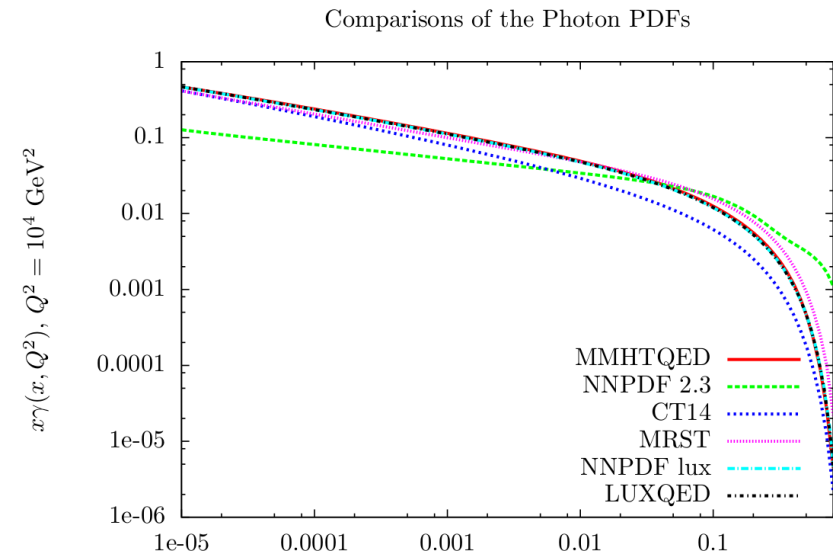
Inelastic and Elastic contributions provided separately.

Modern **LUX**-based PDFs all in excellent agreement with very small uncertainty.

Historical photon PDFs have much more variation.

MMHTqed photon largely in good agreement with **LUXqed**.

Main differences (slightly larger at small x , smaller for $x \sim 0.5$) due to differences in quarks – PDFs not exactly the same as **MMHT2014**.

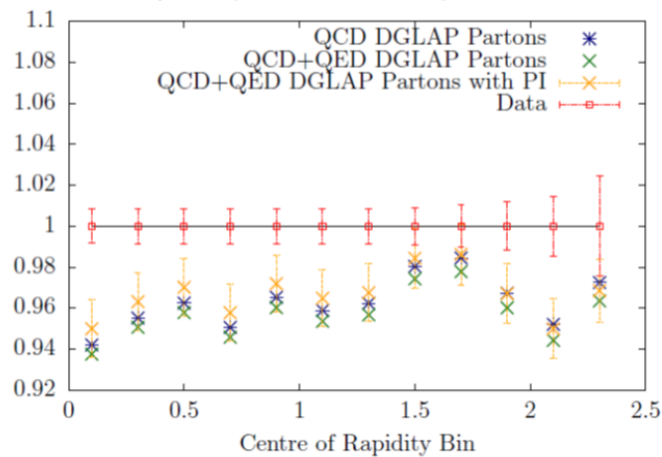


Impact on fit to **ATLAS** high-mass **Drell-Yan** data.

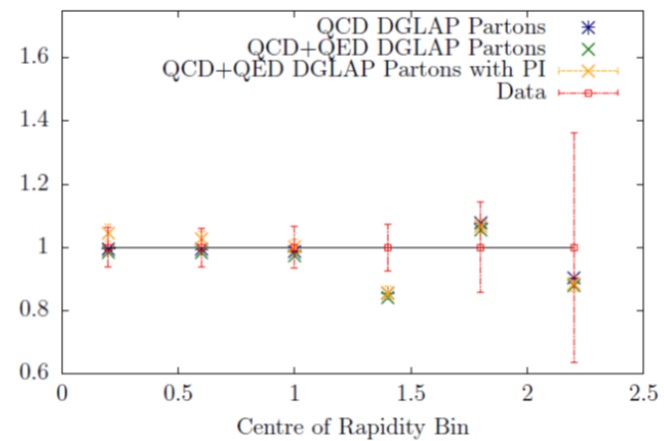
This data no longer constrains the photon in any meaningful way. Fit quality including photon contributions $\chi^2/N_{pts} = 65/48$.

In some bins **QED**-altered evolution of quarks more important than photon contribution.

Theory Prediction/Data (ATLAS 8 TeV 2016), $116 \text{ GeV} < M_{ll} < 150 \text{ GeV}$



Theory Prediction/Data (ATLAS 8 TeV 2016), $500 \text{ GeV} < M_{ll} < 1500 \text{ GeV}$



Conclusions

LHC data starting to have a very significant impact on PDF extractions.

Theory catching up for precision data, e.g. **NNLO** jets, differential top, $Z, W p_T \dots$

Significant changes in strange distribution most likely first major change (uncertainty and central value) and small- x $d_v(x)$.

Improvements in parameterisation. Better fit to data - improves some (not all) data tensions and increases some uncertainties in extreme kinematic regions.

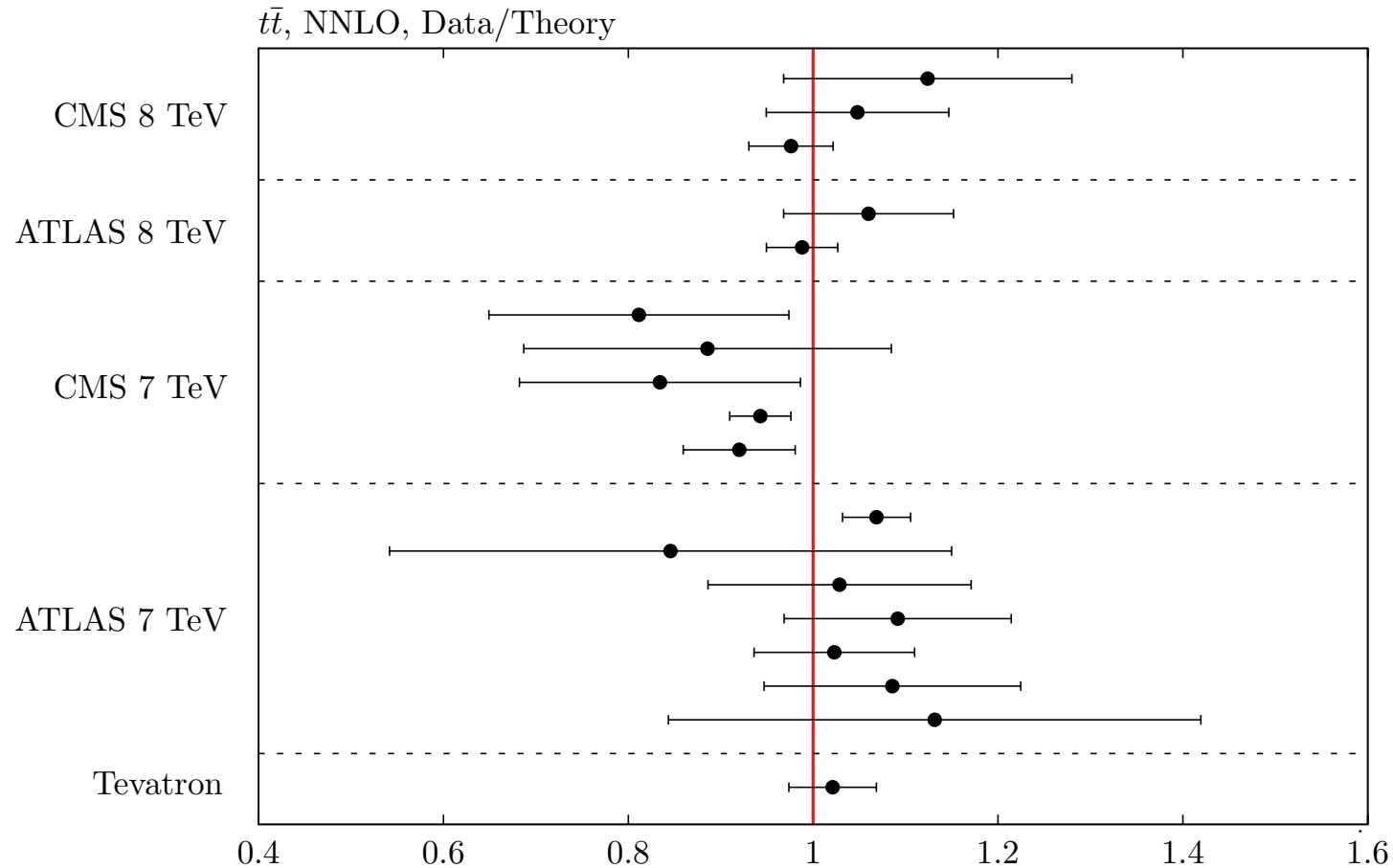
MMHT PDFs with full **QED** corrections complete.

Put everything together (with a “couple” more data sets) for full “**MMHT**”2019 update.

Precision data and theory causing problems in cases where correlated systematics (which increasingly dominate) are important. Improved interplay between theory/experiment on these seems a priority.

Back-up

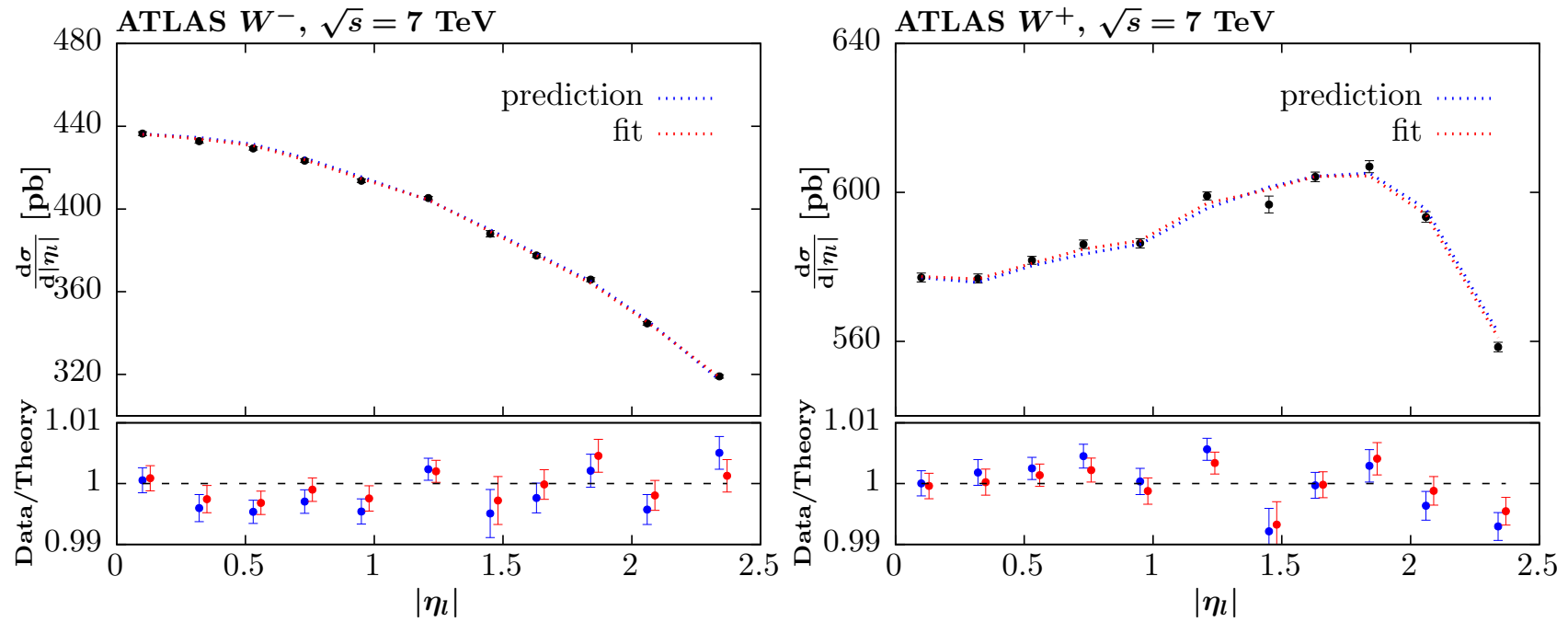
MMHT15 Included some more up-to-date results on $\sigma_{t\bar{t}}$.



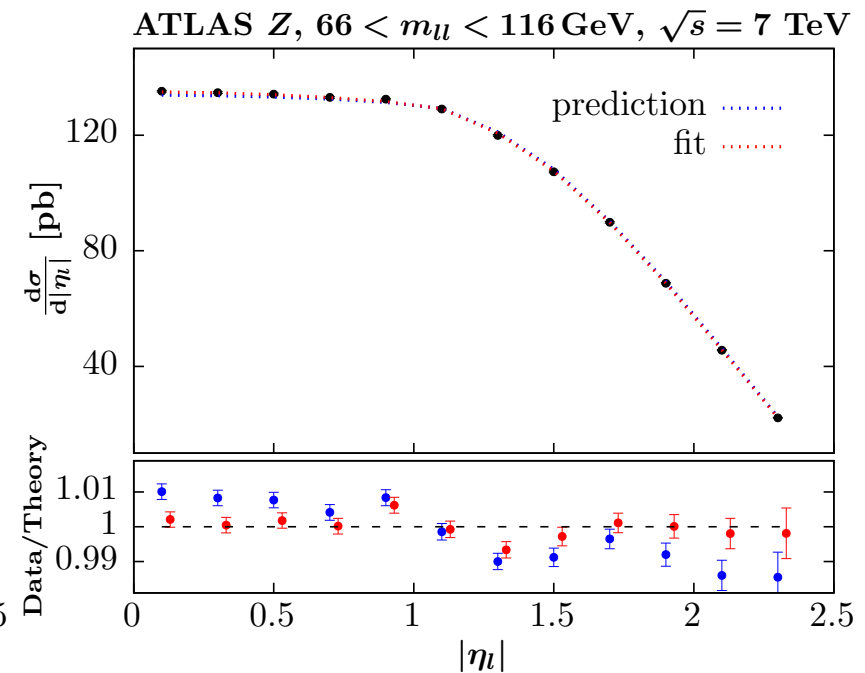
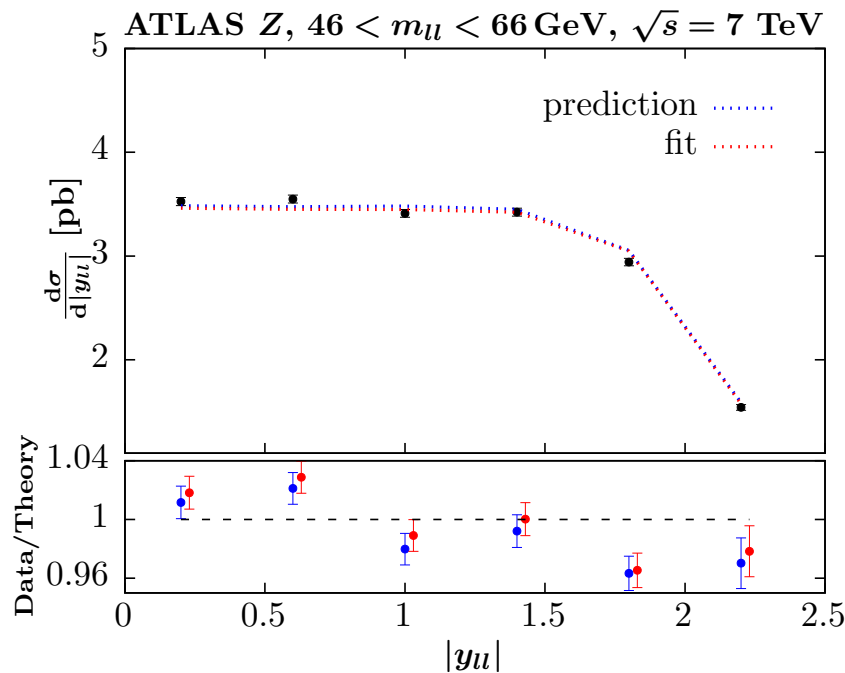
Fit very good and with $\alpha_S(M_Z^2) = 0.118$ the fitted $m_t^{pole} = 173.4$ GeV.
 At NLO $m_t^{pole} = 170.2$ GeV. MMHT values $m_t^{pole} = 174.2$ GeV and $m_t^{pole} = 171.7$ GeV

Helps drive slight increase in $\alpha_S(M_Z^2)$

Prediction and Fit to data



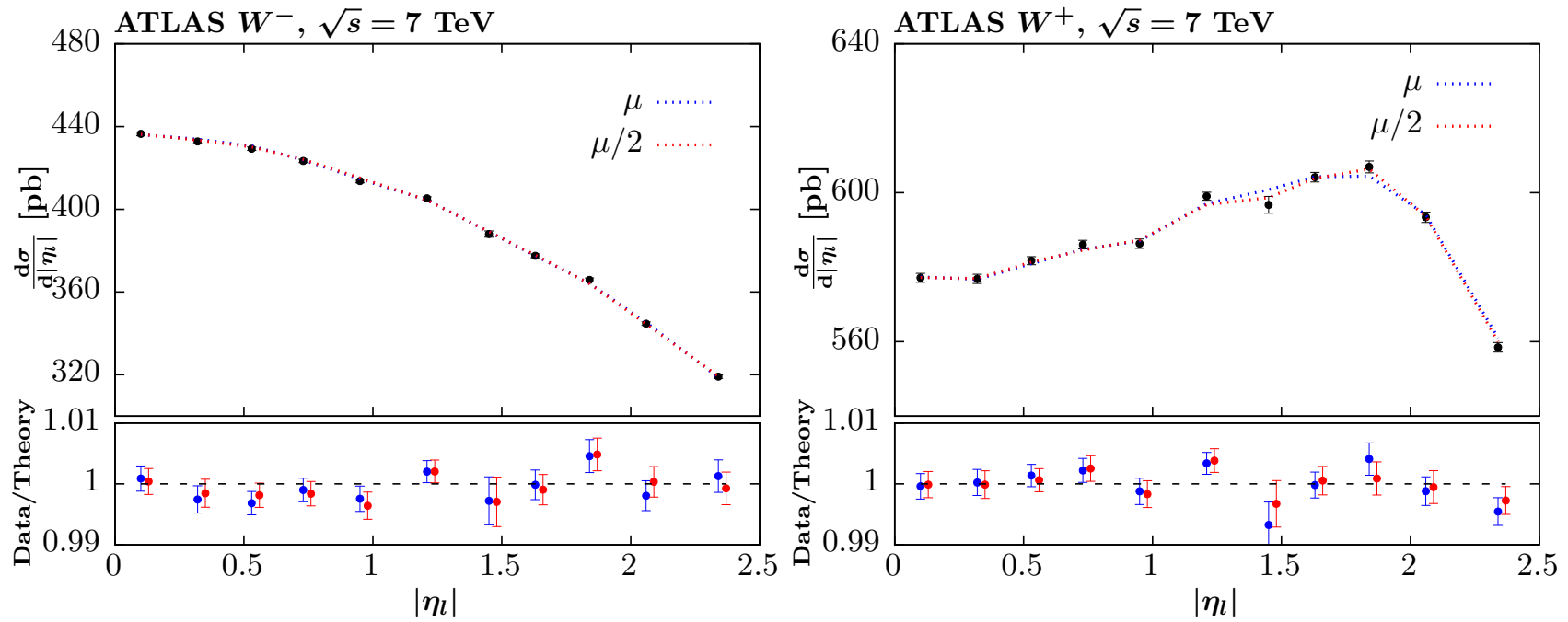
Slight reduction in lower $|\eta|$ W^- required and opposite for W^+ .



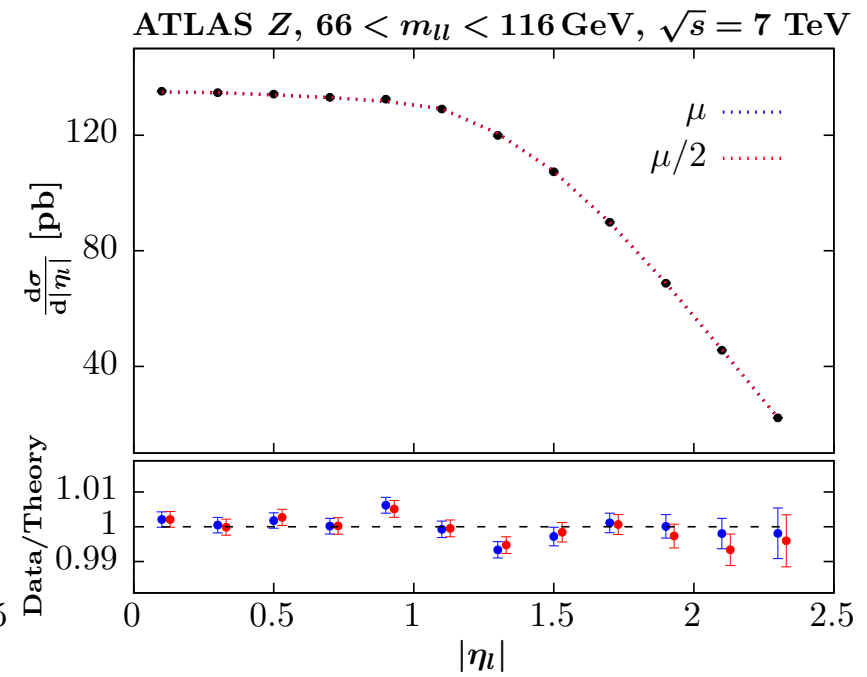
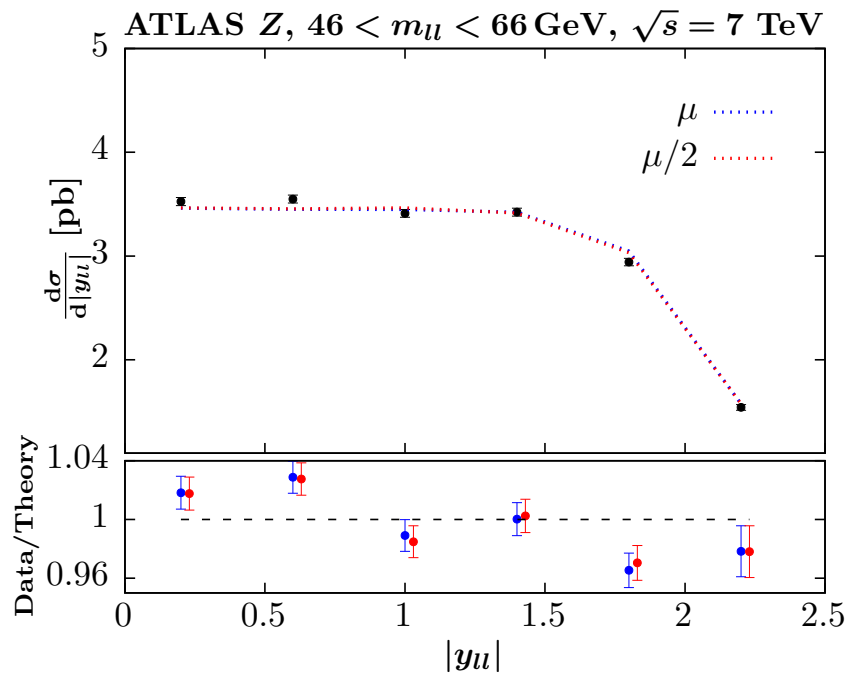
Significant change in shape required for Z production, Higher at low $|\eta|$ and lower at high $|\eta|$

Even with fit difficulty in shape for lower mass data.

Change scales to $\mu_{R,F} = M_{W,Z}/2$



More noticeable improvement for W^+ .



Marginal improvement in shape problem at lower mass.

Less fluctuation for Z peak rapidity distribution.

Studied by **NNPDF** - smaller strange enhancement.

PDF set	$R_s(x = 0.023, Q = 1.65 \text{ GeV})$	$R_s(x = 0.013, Q = M_Z)$
NNPDF3.0	0.47 ± 0.09	0.79 ± 0.04
NNPDF3.1	0.62 ± 0.12	0.83 ± 0.05
NNPDF3.1 collider-only	0.86 ± 0.17	0.94 ± 0.07
NNPDF3.1 HERA + ATLAS W, Z	0.96 ± 0.20	0.98 ± 0.09
ATLAS W, Z 2011 xFitter (Ref. [93])	$1.13^{+0.11}_{-0.11}$	-
ATLAS W, Z 2010 HERAFitter (Ref. [120])	$1.00^{+0.25}_{-0.28} (*)$	$1.00^{+0.09}_{-0.10} (*)$

👤 **Confirmed the strange symmetric fit** preferred by the ATLAS W,Z 2011 measurements, though we find PDF uncertainties larger by a factor 2

👤 The **global fit** accommodates both the neutrino data and the ATLAS W,Z 2011 ($\chi^2_{\text{nutev}}=1.1$, $\chi^2_{\text{AWZ11}}=2.1$) finding a compromise value for $R_s=0.62 \pm 0.12$

👤 **Mild tension** in the global fit (1.5-sigma level at most) when simultaneously included neutrino data, CMS W+charm and ATLAS W,Z 2010+2011

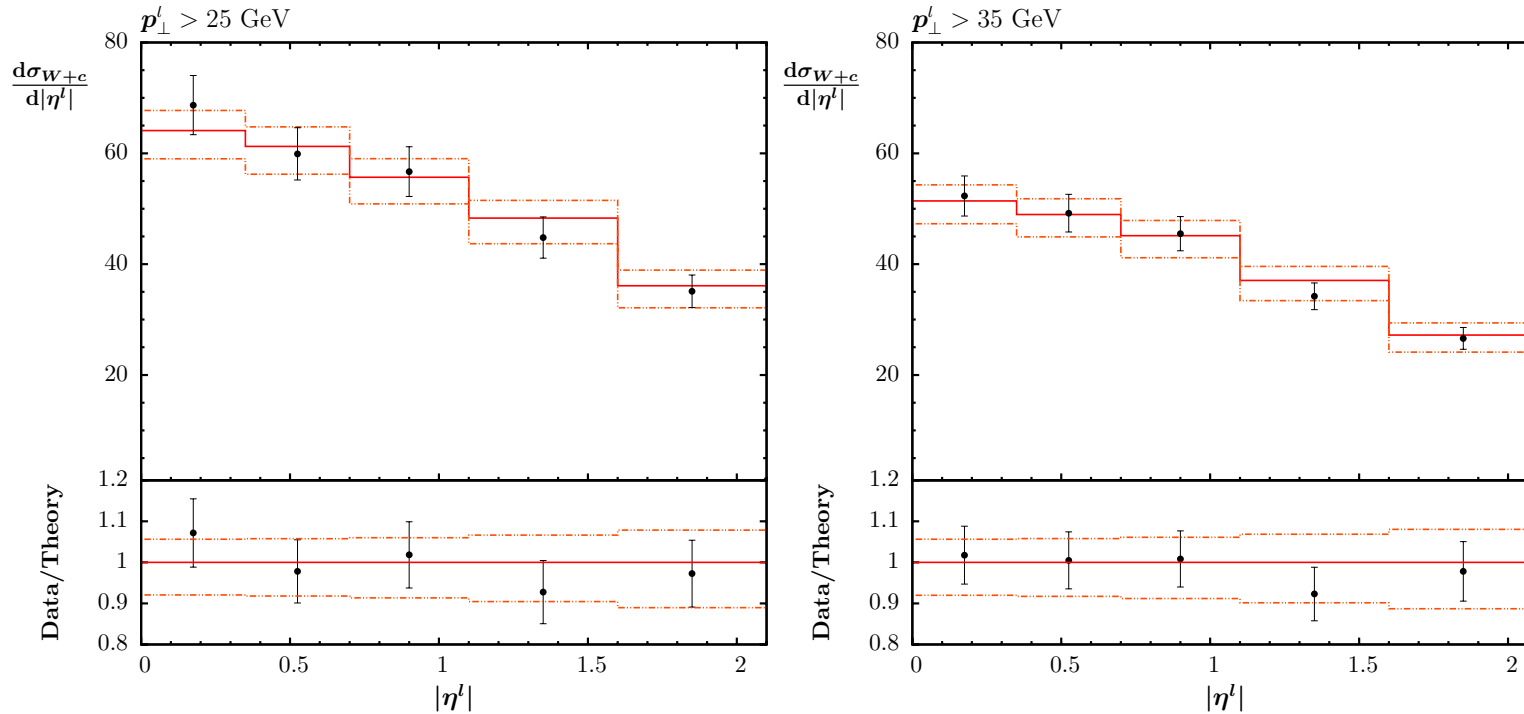
$$\sigma_W \propto c\bar{s}, \quad \sigma_Z \propto g_s * s\bar{s} + g_c * c\bar{c}, \quad \text{where } g_s > g_c.$$

Smaller strange correlated with smaller charm, i.e. σ_Z/σ_W rises with smaller charm.

Improved fit to older **ATLAS W, Z** data with larger m_c evident in **MMHT2014**. Usually interplay with fitting **HERA** data.

Direct constraint on Strange – $W + c$ differential distributions.

	GeV	data	MSTW2008	MMHT2014
$\sigma(W + c)$	$p_T^{\text{lep}} > 25$	$107.7 \pm 3.3(\text{stat.}) \pm 6.9(\text{sys.})$	102.8 ± 1.7	110.2 ± 8.1
$\sigma(W + c)$	$p_T^{\text{lep}} > 35$	$84.1 \pm 2.0(\text{stat.}) \pm 4.9(\text{sys.})$	80.4 ± 1.4	86.5 ± 6.5
R_c^\pm	$p_T^{\text{lep}} > 25$	$0.954 \pm 0.025(\text{stat.}) \pm 0.004(\text{sys.})$	0.937 ± 0.029	0.924 ± 0.026
R_c^\pm	$p_T^{\text{lep}} > 35$	$0.938 \pm 0.019(\text{stat.}) \pm 0.006(\text{sys.})$	0.932 ± 0.030	0.904 ± 0.027



MSTW2008 a bit low (especially for ATLAS), but MMHT2014 seems fine particularly for CMS (shown). Data provides some constraint.

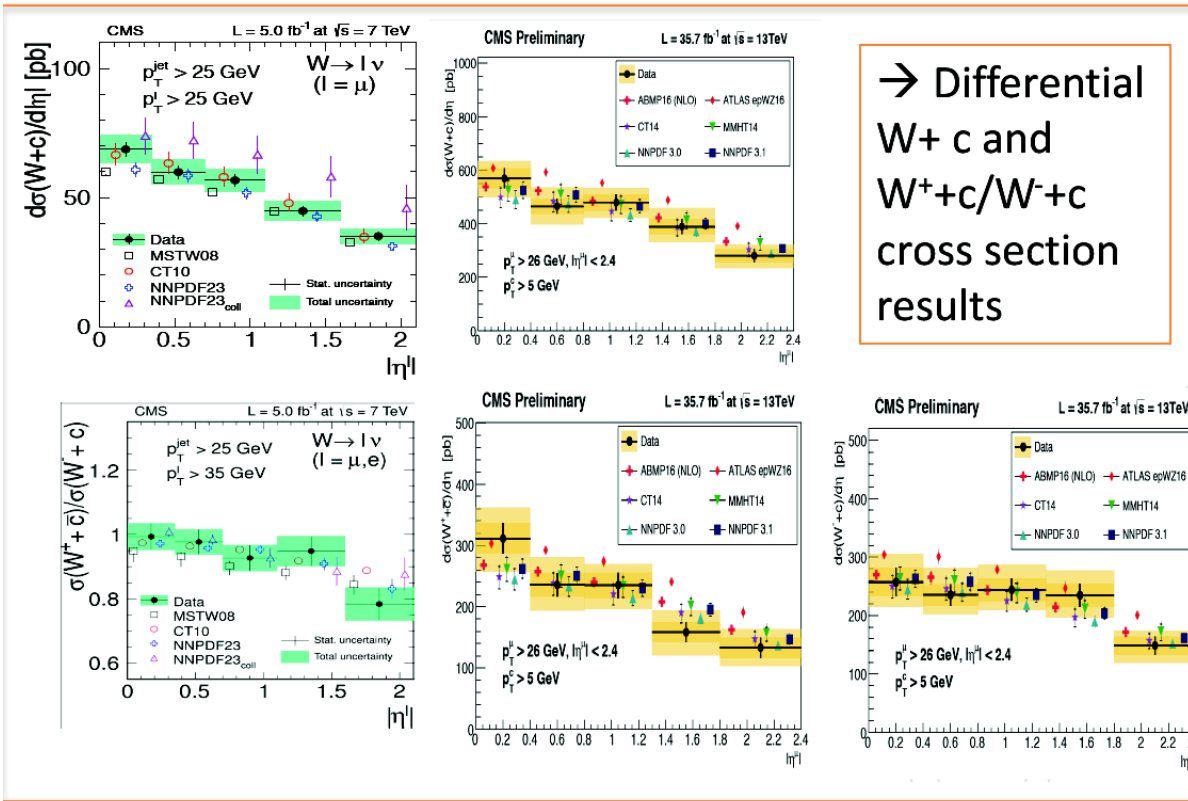
Newer CMS data at 13 TeV – doesn't favour very large $s + \bar{s}$.

NEW

W + c

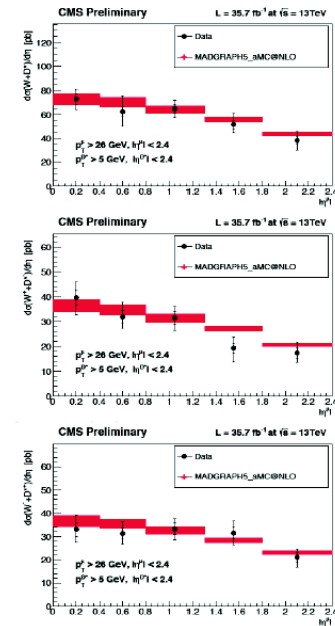
- Measured W + c cross section as well as W⁺+c/W⁻+b ratio
 - inclusively
 - differentially wrt lepton η

**p-p $\sqrt{s}=7,13$ TeV
5,35.7 fb⁻¹**



→ Differential W+ c and W⁺+c/W⁻+c cross section results

- 13TeV: extrapolation to the unmeasured phase space
- As cross check: W + D* x-sec is measured in fiducial range



B. Bilin

DIS 2018

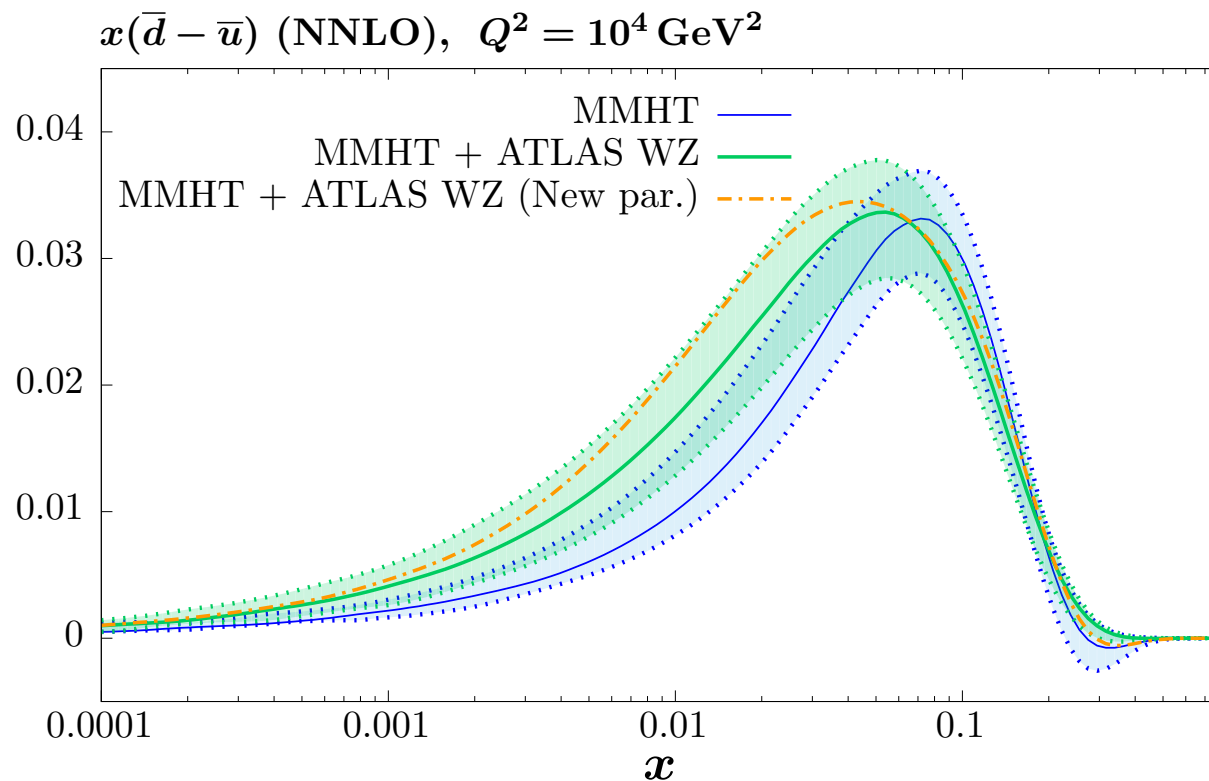
11

For $(\bar{d} - \bar{u})(x, Q_0^2)$ by default use **4** parameters,

$$(\bar{d} - \bar{u})(x, Q_0^2) = A(1 - x)^{\eta_{sea}+2} x^\delta (1 + \gamma x + \Delta x^2),$$

Extend to $(\bar{d} - \bar{u})(x, Q_0^2) = A(1 - x)^{\eta_{sea}+2} x^\delta (1 + \sum_{i=1}^4 a_i T_i(1 - 2x^{\frac{1}{2}}))$,

So **6** free parameters. Easily allows multiple turning points. Improves fit by > 10 points - eases **ATLAS W, Z** and **DY ratio** tension.

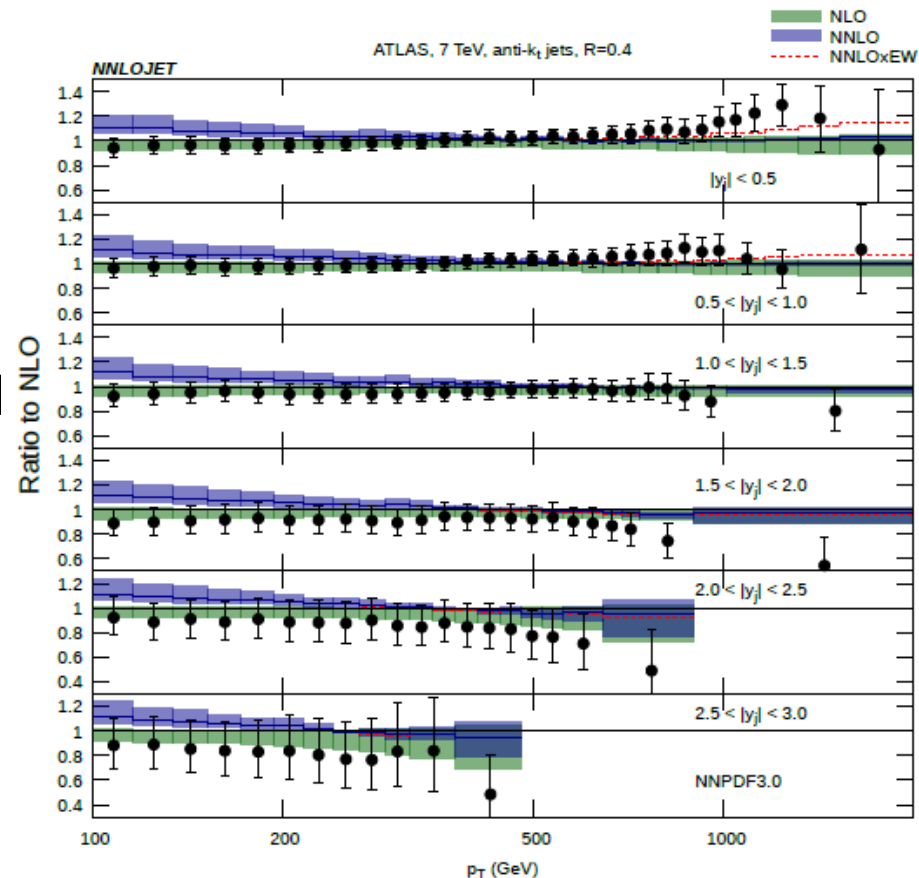


NNLO corrections

Now calculated Currie *et al* / Phys.Rev.Lett. 118 (2017) 072002.

Fit quality can slightly improve or decrease compared to NLO depending on choices.

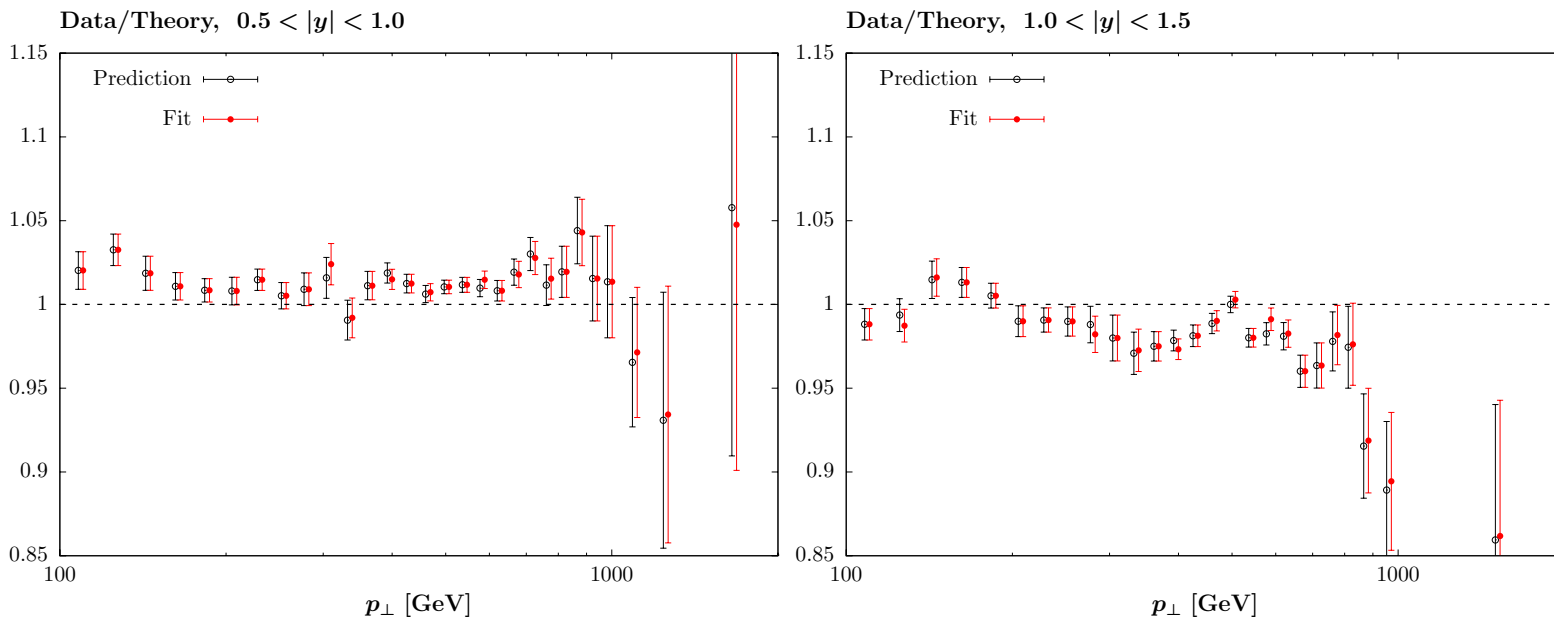
Electroweak corrections to jets different in different bins, but much smaller than systematic effect.



Exact form dependent on R and on scale choice, e.g $\mu = p_{T,1}$ or p_T . Up to 20% at low p_T . Authors now recommend using more physical scale, \hat{p}_T – sum of parton p_T (arXiv:1807.03692), improved convergence criteria properties. Can also resum R dependence Liu, Moch and Ringer – Phys.Rev.Lett. 119 (2017) 212001.

Fit to high luminosity **ATLAS 7 TeV** inclusive jet data – **MMHT** (JHEP 02 (2015) 153)

Difficulty simultaneously fitting data in all rapidity bins. Mismatch in one bin different in form to neighbouring bin constraining PDFs of similar x, Q^2 .



Similar results also seen by other groups.

Qualitative conclusion shown to be independent of jet radius R , choice of scale or inclusion of **NNLO** corrections.

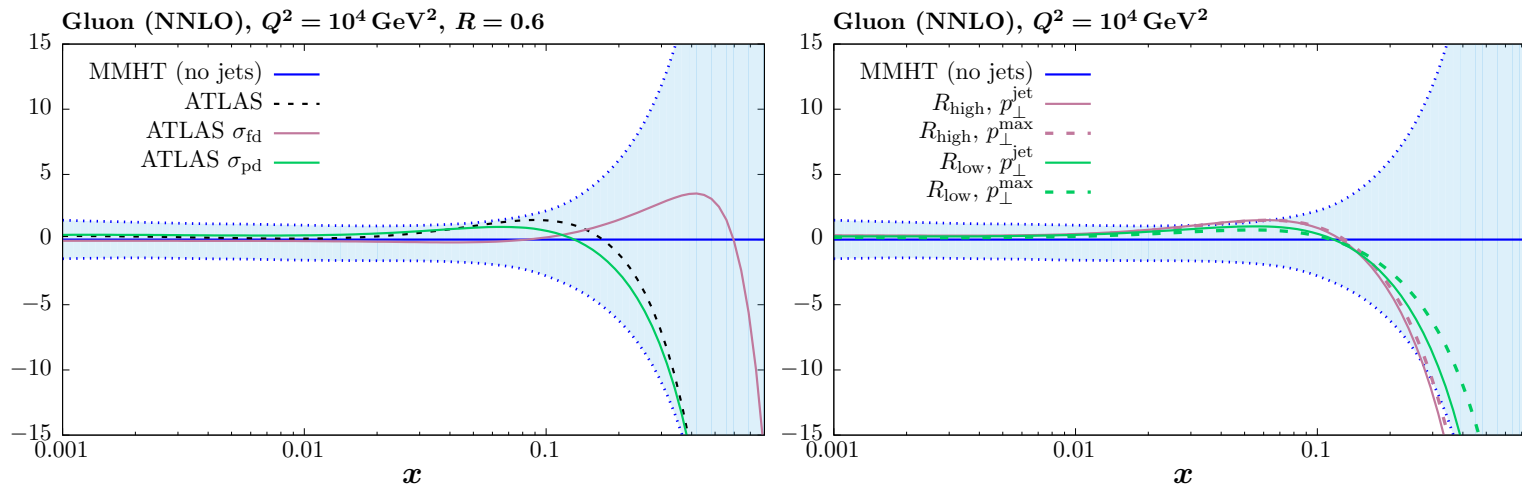
Exercise on decorrelating uncertainties

We consider the effect of decorrelating two uncertainty sources, i.e. making them independent between the 6 rapidity bins. More extensive decorrelation study in [ATLAS – JHEP 09 020 \(2017\)](#).

	Full	21	62	21,62
$\chi^2/N_{\text{pts.}}$	2.85	1.56	2.36	1.27

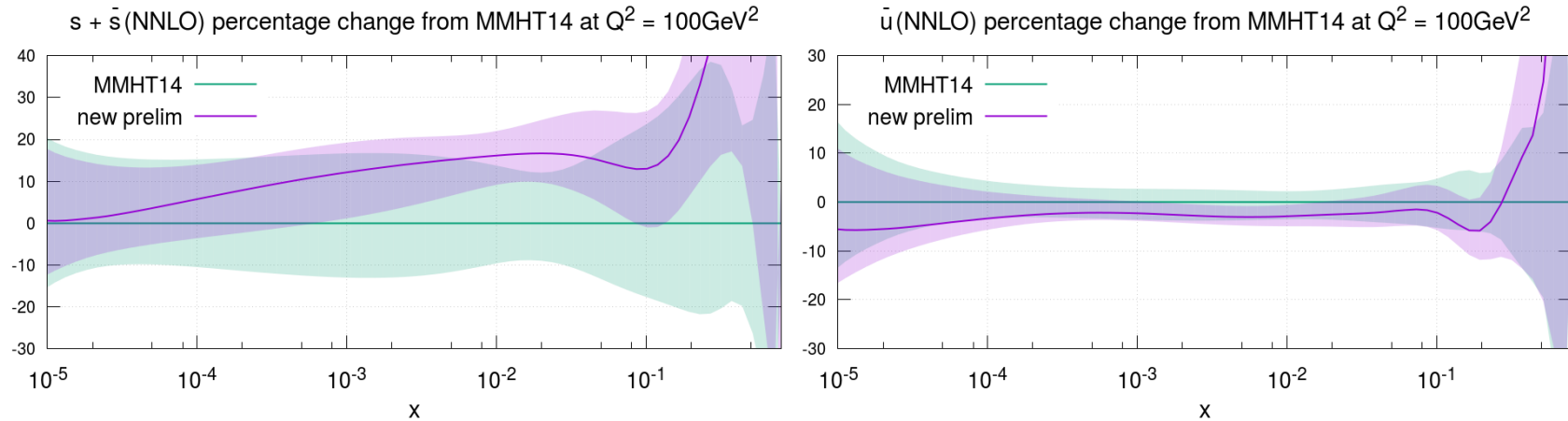
Similar results using new **NNLO** results.

	$R_{\text{low}, p_{\perp}^{\text{jet}}}$	$R_{\text{low}, p_{\perp}^{\text{max}}}$	$R_{\text{high}, p_{\perp}^{\text{jet}}}$	$R_{\text{high}, p_{\perp}^{\text{max}}}$
NLO	210.0 (187.1)	189.1 (181.7)	175.1 (193.5)	164.9 (191.2)
NNLO	172.3 (177.8)	199.3 (187.0)	149.8 (182.3)	152.5 (185.4)



Results insensitive to decorrelation. Find softer gluon, reduced uncertainty. Also relatively little sensitivity to scales and jet radius.

Plots of $s^+(x, Q^2)$ and $\bar{u}(x, Q^2)$



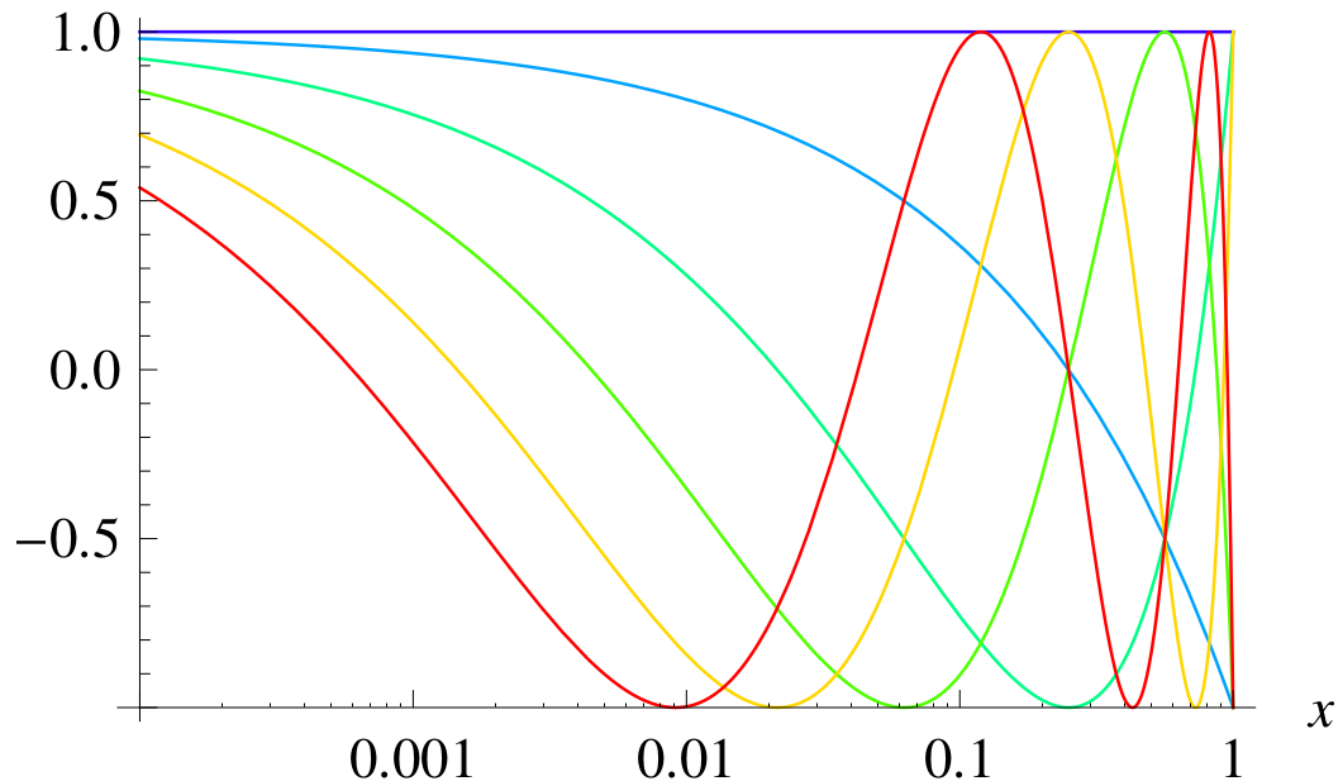
Significant change in shape of $s^+(x, Q^2)$ (note **NNLO** dimuon correction not included here).

Little change in $\bar{u}(x, Q^2)$. Slightly lower due to generally increased $s^+(x, Q^2)$.

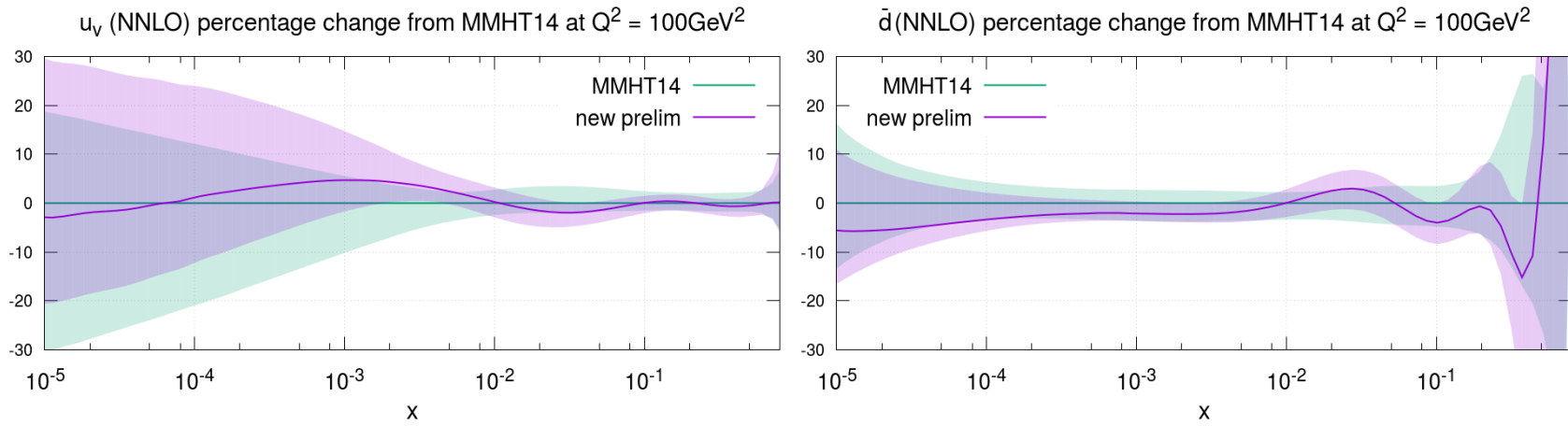
Note – increased uncertainty for $x > 0.6$.

Form of Chebyshev Polynomials.

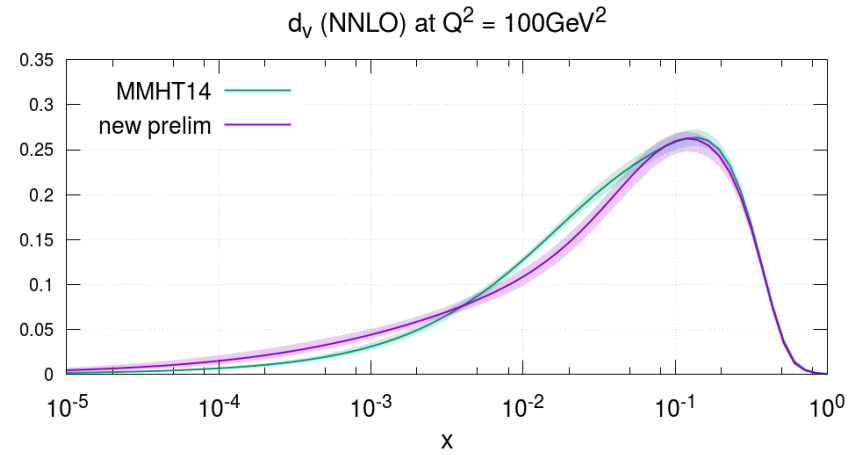
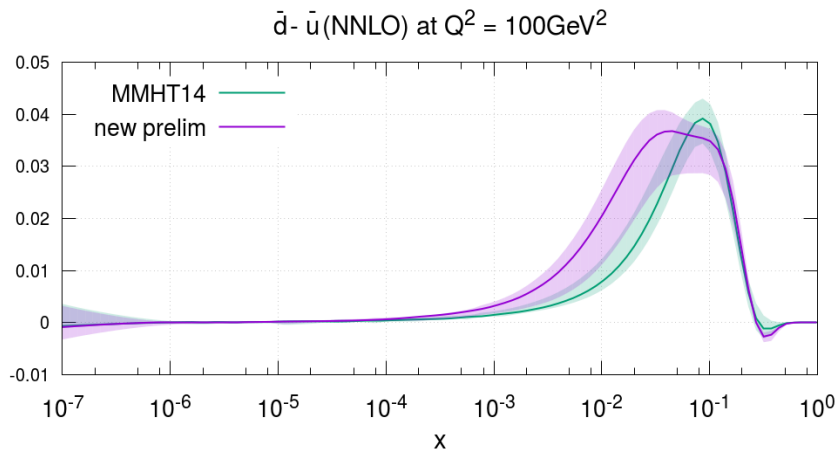
$$T_i(y(x) = 1 - 2\sqrt{x})$$



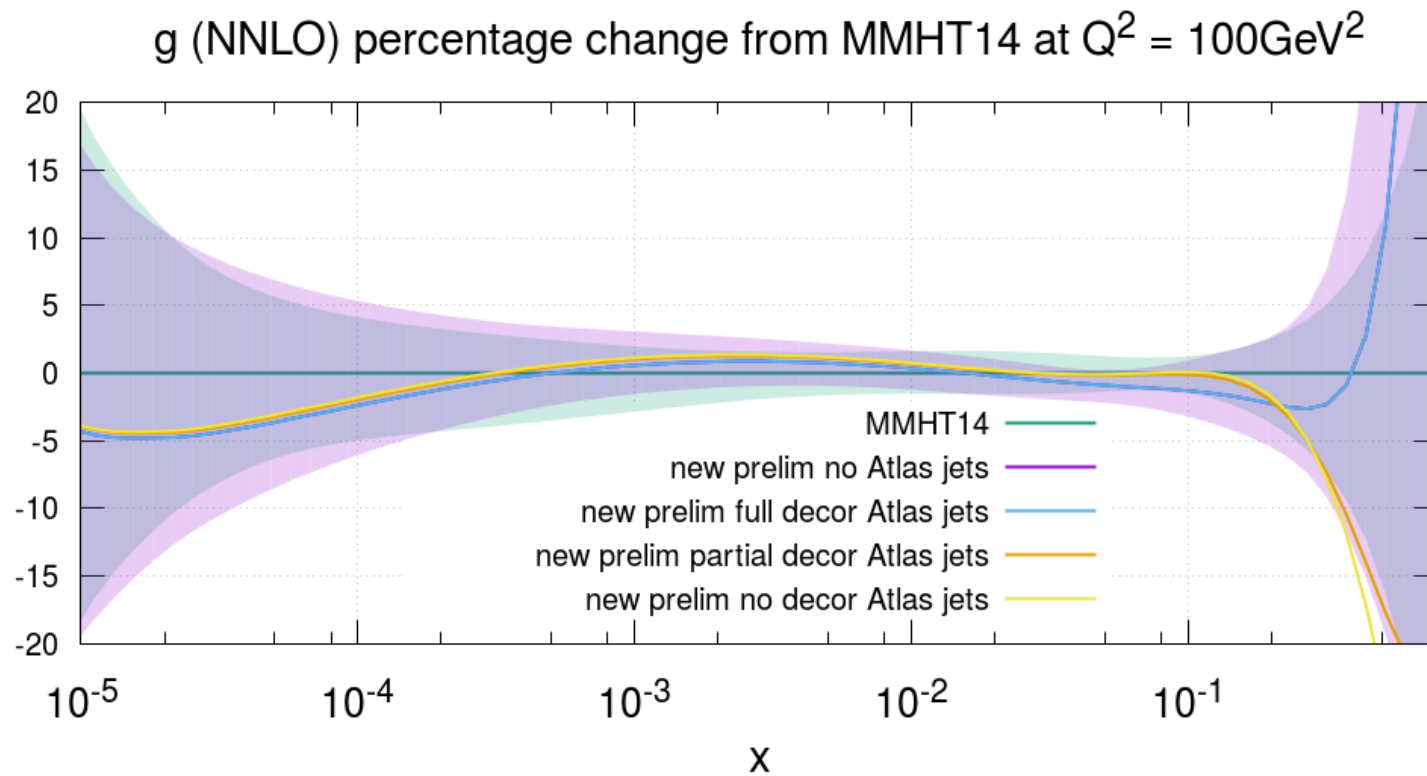
Plots of $u_v(x, Q^2)$ and $\bar{d}(x, Q^2)$



Plots of $d_V(x, Q^2)$ and $\bar{d}(x, Q^2) - \bar{u}(x, Q^2)$.



Impact of **ATLAS** jet data with extended parameterization



Photon PDF in proton

LUXqed photon PDF (A. Manohar et al., PRL 117, 242002 (2016), JHEP 1712, 046 (2017)) relates photon to structure functions.

LUXqed

- Recent study of arXiv:1607.04266:

CERN-TH/2016-155

How bright is the proton?
A precise determination of the photon PDF

Aneesh Manohar,^{1,2} Paolo Nason,³ Gavin P. Salam,^{2,*} and Giulia Zanderighi^{2,4}

¹Department of Physics, University of California at San Diego, La Jolla, CA 92093, USA

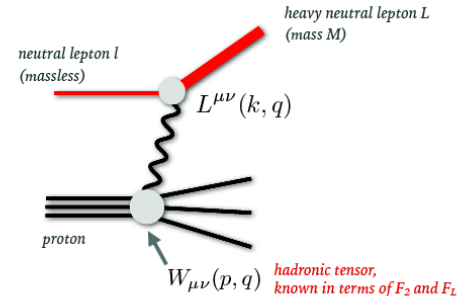
²CERN, Theoretical Physics Department, CH-1211 Geneva 23, Switzerland

³INFN, Sezione di Milano Bicocca, 20126 Milan, Italy

⁴Rudolf Peierls Centre for Theoretical Physics, 1 Keble Road, University of Oxford, UK

- Show how photon PDF can be expressed in terms of F_2 and F_L . Use measurements of these to provide well constrained LUXqed photon PDF.

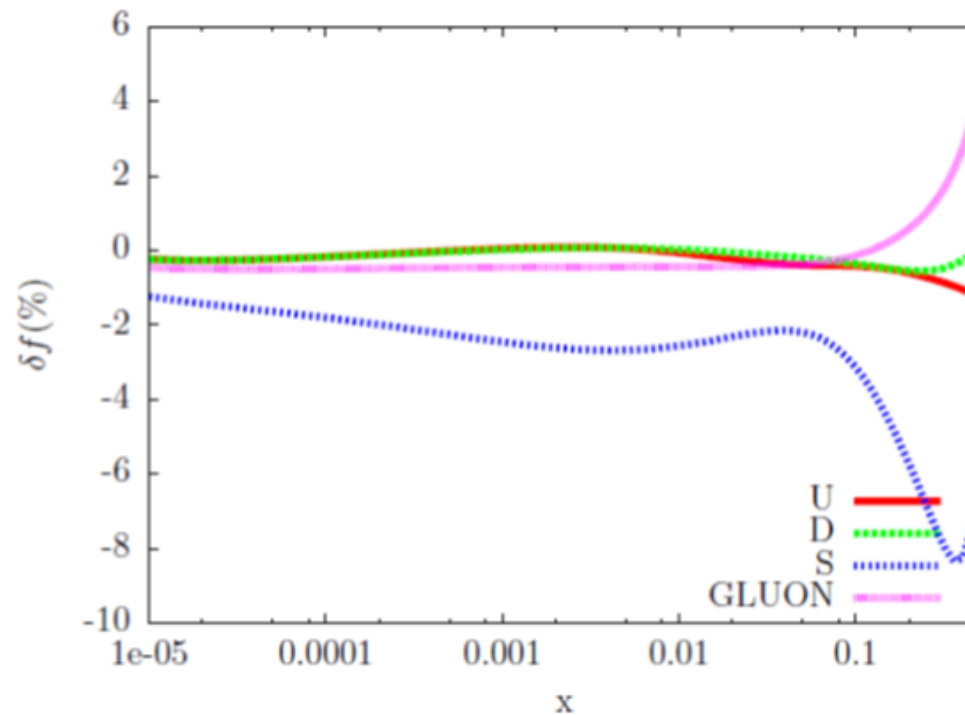
$$x f_{\gamma/p}(x, \mu^2) = \frac{1}{2\pi\alpha(\mu^2)} \int_x^1 \frac{dz}{z} \left\{ \int_{\frac{x^2 m_p^2}{1-z}}^{\frac{\mu^2}{1-z}} \frac{dQ^2}{Q^2} \alpha^2(Q^2) \left[\left(z p_{\gamma q}(z) + \frac{2x^2 m_p^2}{Q^2} \right) F_2(x/z, Q^2) - z^2 F_L\left(\frac{x}{z}, Q^2\right) \right] - \alpha^2(\mu^2) z^2 F_2\left(\frac{x}{z}, \mu^2\right) \right\}, \quad (6)$$



22

Breakdown into well-known elastic (coherent) contribution and moderately model dependent inelastic part Harland-Lang et al. PRD94 (2016) 074008 and earlier studies.

Change in PDFs due to refit

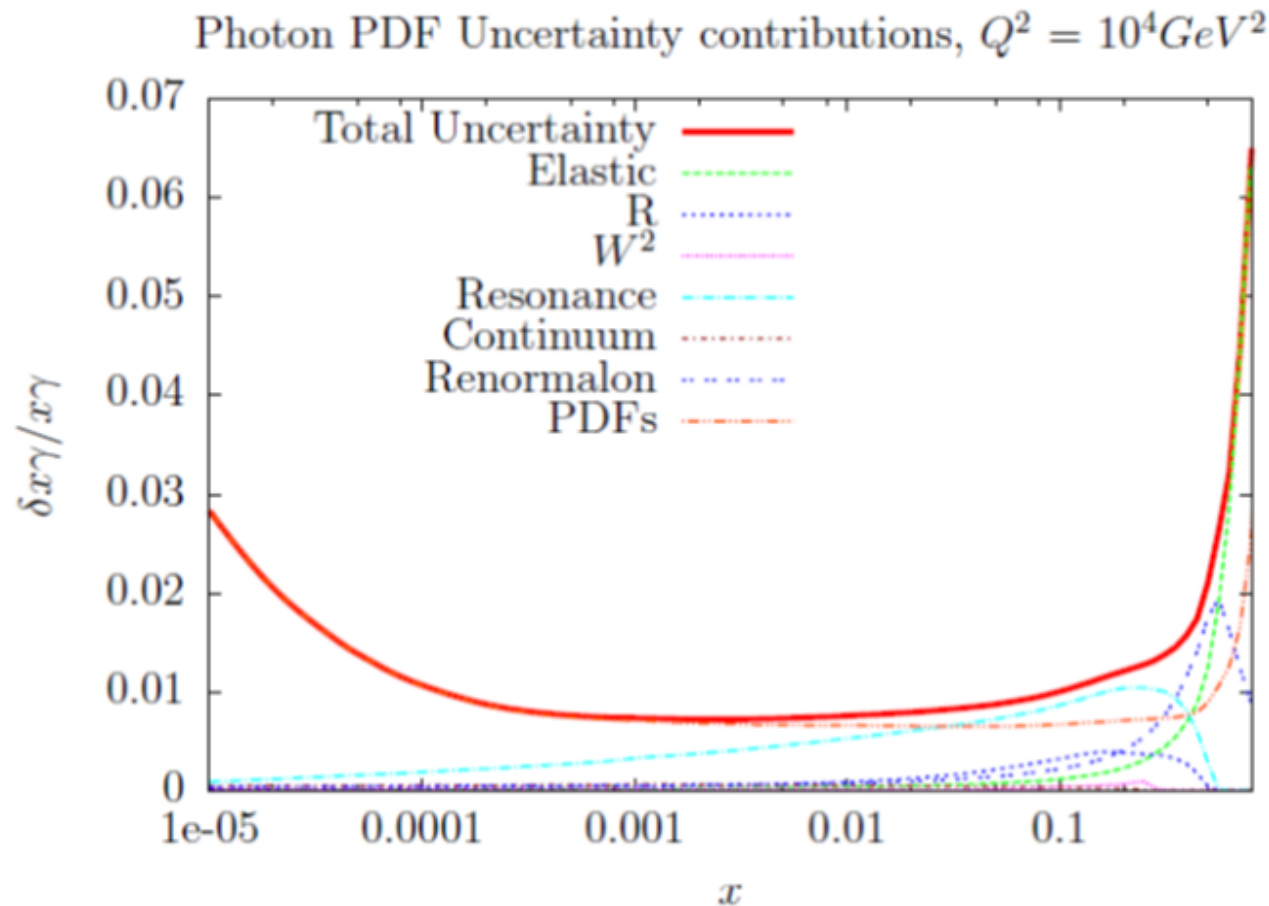


Gluon affected mainly at high x , loss of momentum.

Small x flavour rearrangement in quarks – less strange. Well within uncertainty.

Quarks lose momentum at high x from QED evolution, but reduction in high Q^2 up quark less as compensated for by input.

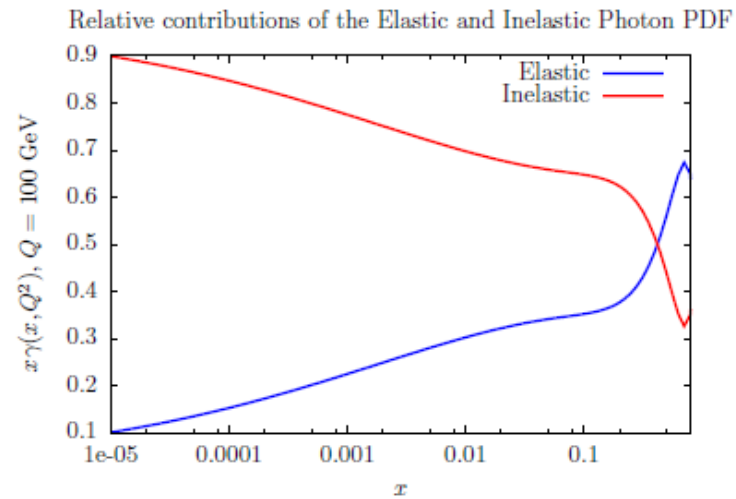
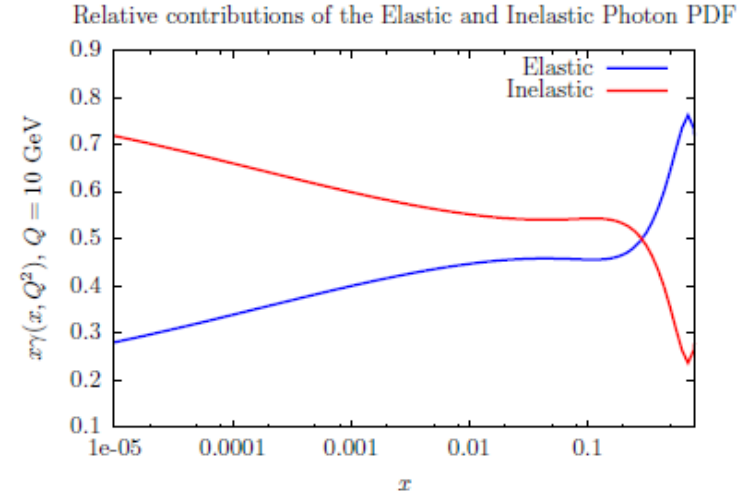
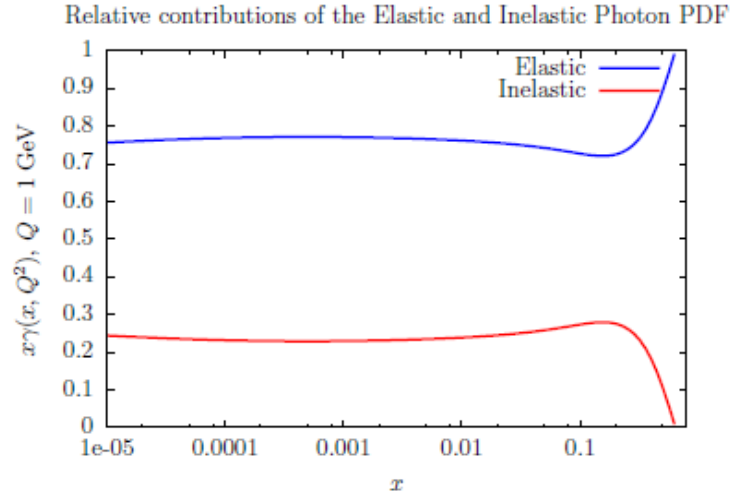
Uncertainties in Photon Distribution



As with **LUXqed** mainly due to PDFs and elastic contribution and the resonance region.

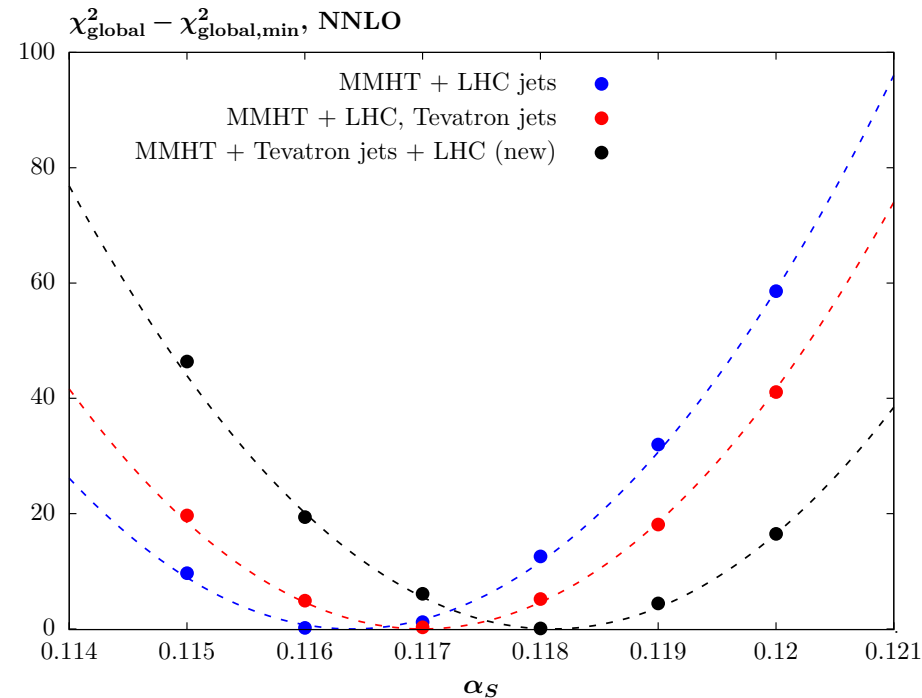
But also a large contribution at high x from higher twist contributions for $Q^2 > Q_0^2$.

Inelastic and Elastic contributions provided separately.



For **MMHT2014** $\alpha_S(M_Z^2) = 0.1172 \pm 0.0013$ ($\alpha_S(M_Z^2) = 0.1178$ when world average added as data point). With **8 TeV** data on $\sigma_{t\bar{t}}$ and final **HERA** data went to $\alpha_S(M_Z^2) = 0.118$.

For further addition of **LHC** jets and removal of **Tevatron** jet data, $\alpha_S(M_Z^2) = 0.1164$. When Tevatron jets also added back $\alpha_S(M_Z^2) = 0.1173$



Also look at inclusion of newer W, Z data from **ATLAS, CMS, LHCb**. Without newer **LHC** jet data $\alpha_S(M_Z^2) = 0.1179$ but with these data $\alpha_S(M_Z^2) = 0.1176$.